© 2014. Published by The Company of Biologists Ltd | Development (2014) 141, 281-295 doi:10.1242/dev.093690

RESEARCH ARTICLE

STEM CELLS AND REGENERATION

Numb family proteins are essential for cardiac morphogenesis and progenitor differentiation

Chen Zhao[1,*], Hua Guo[1,*], Jingjing Li[1], Thomas Myint[1], William Pittman[1], Le Yang[1], Weimin Zhong[2], Robert J. Schwartz[3], John J. Schwarz[1], Harold A. Singer[1], Michelle D. Tallquist[4] and Mingfu Wu[1,‡]

ABSTRACT

Numb family proteins (NFPs), including Numb and numb-like (Numbl), are cell fate determinants for multiple progenitor cell types. Their functions in cardiac progenitor differentiation and cardiac morphogenesis are unknown. To avoid early embryonic lethality and study NFP function in later cardiac development, *Numb* and *Numbl* were deleted specifically in heart to generate myocardial double-knockout (MDKO) mice. MDKOs were embryonic lethal and displayed a variety of defects in cardiac progenitor differentiation, cardiomyocyte proliferation, outflow tract (OFT) and atrioventricular septation, and OFT alignment. By ablating NFPs in different cardiac populations followed by lineage tracing, we determined that NFPs in the second heart field (SHF) are required for OFT and atrioventricular septation and OFT alignment. MDKOs displayed an SHF progenitor cell differentiation defect, as revealed by a variety of methods including mRNA deep sequencing. Numb regulated cardiac progenitor cell differentiation in an endocytosis-dependent manner. Studies including the use of a transgenic Notch reporter line showed that Notch signaling was upregulated in the MDKO. Suppression of Notch1 signaling in MDKOs rescued defects in p57 expression, proliferation and trabecular thickness. Further studies showed that Numb inhibits Notch1 signaling by promoting the degradation of the Notch1 intracellular domain in cardiomyocytes. This study reveals that NFPs regulate trabecular thickness by inhibiting Notch1 signaling, control cardiac morphogenesis in a Notch1-independent manner, and regulate cardiac progenitor cell differentiation in an endocytosis-dependent manner. The function of NFPs in cardiac progenitor differentiation and cardiac morphogenesis suggests that NFPs might be potential therapeutic candidates for cardiac regeneration and congenital heart diseases.

KEY WORDS: Numb family proteins, Cardiac progenitor cell, Cardiac morphogenesis, Mouse

INTRODUCTION

Congenital heart defects (CHDs) occur in ~1% of live births (Hoffman and Kaplan, 2002), yet knowledge of the underlying genetic causes of the specific structural defects involved is still limited (Olson, 2006; Bruneau, 2008). Moreover, the lack of understanding of how cardiac progenitor cells renew and differentiate *in vivo* has impeded progress toward treating cardiovascular disease by cardiac regeneration using endogenous cardiac progenitors.

Drosophila Numb, an intracellular adaptor protein, was the first molecule discovered to influence cell fate by its asymmetric segregation during cell division (Rhyu et al., 1994) and by inhibiting Notch signaling (Uemura et al., 1989; Frise et al., 1996; Spana and Doe, 1996; Petersen et al., 2002). In mice, Numb has two homologs, Numb and numb-like (Numbl), collectively known as Numb family proteins (NFPs). NFPs are nearly ubiquitously expressed during embryogenesis (Zhong et al., 1997) and are known to function as cell fate determinants by maintaining neural stem cell fate and regulating its differentiation (Verdi et al., 1996; Petersen et al., 2002; Li et al., 2003; Petersen et al., 2004). NFPs are also involved in the specification and differentiation of hematopoietic stem cells (Wu et al., 2007), muscle satellite cells (Conboy and Rando, 2002), cancer stem cells (Ito et al., 2010) and hemangioblasts (Cheng et al., 2008). Recently, additional mechanisms of Numb signaling at the molecular level have been revealed. Numb functions as a component of the adherens junction to regulate cell adhesion and migration (Rasin et al., 2007; Wang et al., 2009; Wu et al., 2010), and is involved in the ubiquitylation of p53 (Trp53) (Colaluca et al., 2008) and Gli1 (Di Marcotullio et al., 2006) to regulate cancer initiation. Numb has also been reported to complex with β-catenin (Rasin et al., 2007; Wu et al., 2010; Kwon et al., 2011) to regulate Wnt signaling. Additionally, Numb interacts with integrin β subunits (Calderwood et al., 2003) and promotes their endocytosis for directional cell migration (Nishimura and Kaibuchi, 2007).

Cardiac development is a spatiotemporally regulated multistep morphogenetic process that depends on the addition of progenitor cells from four different sources, including cells from the first heart field and second heart field (FHF and SHF), cells derived from cardiac neural crest cells (CNCCs) and cells derived from the pro-epicardial organ (Kelly et al., 2001; Mjaatvedt et al., 2001; Waldo et al., 2001; Verzi et al., 2005; Vincent and Buckingham, 2010). The SHF progenitor cells migrate to the pre-existing scaffold of the linear heart tube and contribute to the right ventricle, outflow tract (OFT) myocardium and to some endocardium at embryonic day (E) 8.5-10.25 (Kelly and Buckingham, 2002; Buckingham et al., 2005; Verzi et al., 2005; Ward et al., 2005). Perturbation of SHF deployment and progenitor differentiation leads to a spectrum of CHDs (Kelly, 2012) and is responsible for the majority of CHDs (Buckingham et al., 2005; Bruneau, 2008). The posterior SHF contributes to the dorsal mesenchymal protrusion (DMP), an essential structure for chamber septation (Snarr et al., 2007a). Abnormal differentiation and development of the posterior SHF has been associated with cardiac morphogenesis defects, such as atrial septal defect (ASD) and atrioventricular septal defect (AVSD) (Briggs et al., 2012). However, the molecules and the mechanisms that regulate posterior SHF development are not entirely clear.

[1]Cardiovascular Science Center, Albany Medical College, Albany, NY 12208, USA. [2]Molecular, Cellular and Developmental Biology, Yale University, New Haven, CT 06520, USA. [3]Biology and Biochemistry, University of Houston, Houston, TX 77204-5001, USA. [4]JABSOM, Center for Cardiovascular Research, University of Hawaii, Honolulu, HI 96813, USA.
*These authors contributed equally to this work

‡Author for correspondence (wum@mail.amc.edu)

Received 1 January 2013; Accepted 21 October 2013

Development (2014) doi:10.1242/dev.093690

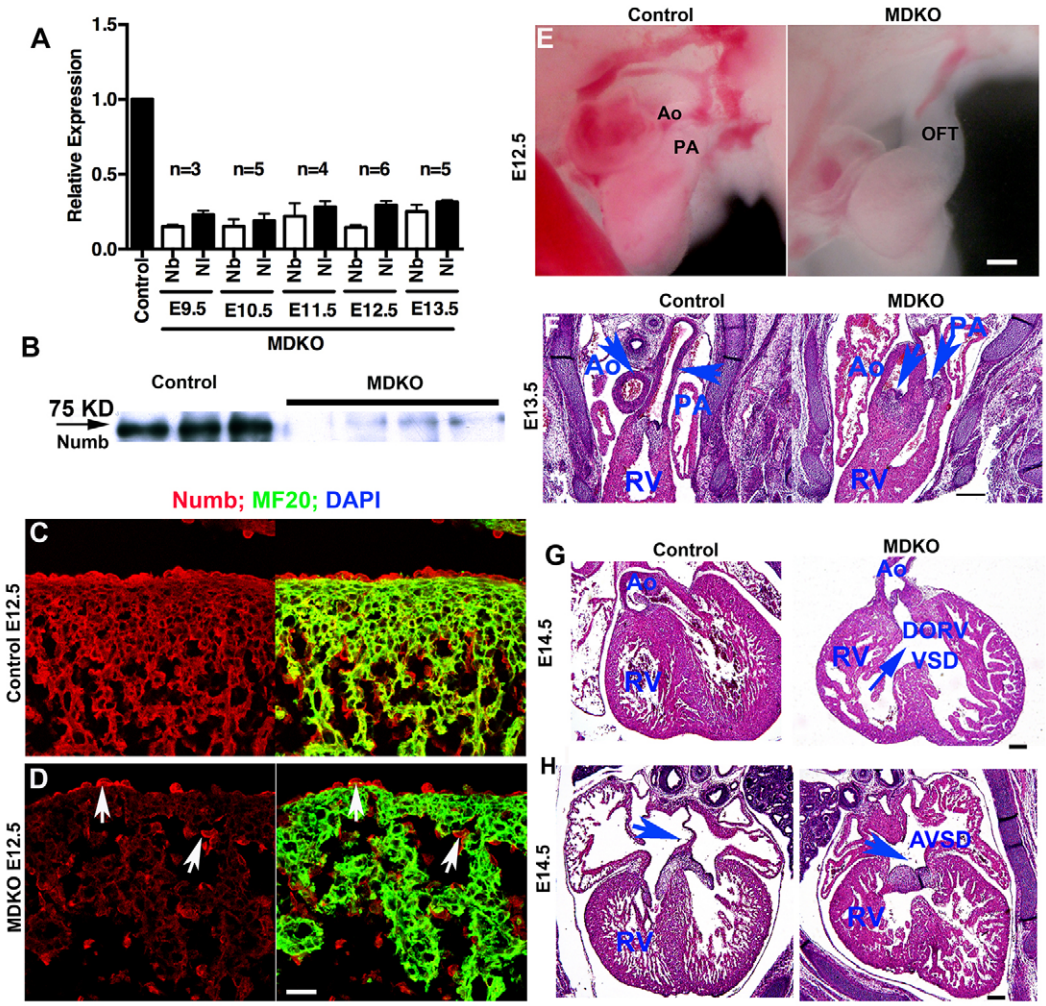

Fig. 1. MDKO hearts display a variety of morphogenetic defects. (A) *Numb* (Nb) and *Numbl* (Nl) deletions in the MDKO and control mouse hearts at different embryonic stages were examined by Q-PCR. The control is set at 1.0. (B) *Numb* deletion in the MDKO was confirmed by western blot using E12.5 ventricles. (C,D) Numb was deleted in cardiomyocytes, but not in epicardial and endothelial cells (arrows). (E) MDKO hearts displayed an outflow tract (OFT) delayed septation defect at E12.5. (F) MDKO hearts displayed pulmonary artery and aortic alignment defects, with both aortic and pulmonary valves in the same plane and both arteries extending from the right ventricle (RV). The blue arrows indicate aorta (Ao), pulmonary artery (PA) and their valves. (G,H) MDKO displayed double outlet right ventricle (DORV) and atrioventricular septal defect (AVSD), as indicated by the blue arrows. Scale bars: 50 μm in C,D; 100 μm in E-H.

Knowledge of NFP function in the mammalian heart is limited and the specific role of NFPs in cardiac development is still unclear. In *Drosophila*, Numb is implicated in controlling myogenic cell fate by interfering with Notch signaling (Han and Bodmer, 2003). In zebrafish, Numb is required for heart left-right asymmetric morphogenesis via regulation of Notch signaling (Niikura et al., 2006). In mice, Numb is reportedly expressed in adult cardiac progenitor cells and is asymmetrically distributed during progenitor asymmetric division (Cottage et al., 2010; Mishra et al., 2011). Additionally, we have shown that NFPs are essential for epicardial cells entering into myocardium (Wu et al., 2010). Very recent work has shown that NFPs regulate myocardial compaction by inhibiting Notch2 (Yang et al., 2012).

We previously reported that conditional deletion of NFPs in epicardial cells caused epicardial cell epithelial-mesenchymal transition defects (Wu et al., 2010). In this study, we deleted NFPs via *Nkx2.5*$^{Cre/+}$ to generate *Numb* and *Numbl* myocardial double-knockout (MDKO) mice, and found that NFPs are required for myocardial trabeculation, cardiac progenitor cell differentiation, cardiomyocyte proliferation, OFT and atrioventricular septation and OFT alignment. Deletion of NFPs in the SHF recapitulated the morphogenetic defects of the MDKO. Further biochemical and genetic studies revealed that Notch1 signaling is upregulated in the myocardium of MDKOs and suppression of Notch1 signaling partially rescued the defects of trabeculation and proliferation in MDKOs. In summary, NFPs inhibit Notch1 to regulate cardiomyocyte proliferation and trabecular thickness, and mediate cardiac progenitor cell differentiation in an endocytosis-dependent, Notch1-independent manner.

RESULTS

NFPs are essential for cardiac development and morphogenesis

Numb and *Numbl* were deleted in mouse heart by *Nkx2.5*$^{Cre/+}$, which is active in myocardium (Moses et al., 2001) and some endocardial cells based on the *Rosa26-mTmG* (mTmG) reporter line (supplementary material Fig. S1A-C, Movie 1) (Muzumdar et al., 2007). We refer to these mice as *Numb* and *Numbl* myocardial double knockout (MDKO). Loss of expression of *Numb* and *Numbl* in E9.5-13.5 MDKO ventricles was 70-90% as determined by Q-PCR (Fig. 1A) and western blot (Fig. 1B). Immunofluorescence (IF) staining confirmed the deletion of Numb in the myocardium of the MDKO (Fig. 1C,D) and indicated that the 10-30% residual expression was due to Numb expression in epicardial and endocardial cells (Fig. 1C,D).

No MDKO animals from 20 litters survived to birth, whereas deletion of up to three alleles of *Numb* and *Numbl* in any combination resulted in animals that survived to adulthood and displayed no gross morphological or cardiac morphogenetic defects (Table 1; supplementary material Fig. S1D), indicating that Numb

Development (2014) doi:10.1242/dev.093690

Table 1. Survival rate of MDKO mice and embryos

Age	*n*	Heterozygous	MDKO	Harvested/expected percentage of MDKO
P1 or older	124	30	0	0/25
E15.5-18.5	260	68	15	6/25
E14.5	182	46	18	10/25
E13.5	320	82	53	17/25
E12.5	355	88	69	19/25
E11.5	320	79	82	25/25
E10.5	426	106	108	25/25
E9.5	226	56	54	25/25

Data were generated from a minimum of 20 litters at each time point. *Nkx2.5-Cre*$^{+/-}$*; Numb*$^{fl/+}$*; Numbl*$^{fl/fl}$ or *Nkx2.5-Cre*$^{+/-}$*; Numb*$^{fl/fl}$*; Numbl*$^{fl/+}$ males were crossed to *Numb*$^{fl/fl}$*; Numbl*$^{fl/fl}$ females to generate the MDKO. *Nkx2.5-Cre*$^{+/-}$*; Numb*$^{fl/+}$*; Numbl*$^{fl/fl}$ and *Nkx2.5-Cre*$^{+/-}$*; Numb*$^{fl/fl}$*; Numbl*$^{fl/+}$ are designated as heterozygous and *Nkx2.5-Cre*$^{+/-}$*; Numb*$^{fl/fl}$*; Numbl*$^{fl/fl}$ is designated as MDKO.
n, total number of offspring or embryos.

and Numbl function redundantly during cardiac morphogenesis. MDKO embryos were indistinguishable from their littermates until E12.5, at which point they began to show edema that became more severe at E13.5 (supplementary material Fig. S1E,F).

MDKO hearts displayed a variety of morphogenetic defects. By E11.5, MDKO heart size was larger than that of the control and the OFT of MDKO hearts exhibited abnormal alignment with the right ventricle (supplementary material Fig. S1G). At E12.5, the aortic and pulmonary artery in the distal OFT (Webb et al., 2003) were separated in control but not in MDKO hearts, indicating an OFT septation defect (Fig. 1E, Table 2). At E13.5, the aorta and pulmonary artery in MDKO hearts were finally separated, but displayed an alignment defect with the aortic and pulmonary valves being in the same plane (Fig. 1F). The alignment defect at E14.5 in MDKOs was visible by gross morphology as both aortic and pulmonary arteries extended from the right ventricle in a parallel pattern (supplementary material Fig. S1H), which resulted in a double outlet right ventricle (DORV) (Fig. 1G, Table 2). MDKO hearts also displayed an AVSD, permitting both atrial and ventricular shunting (Fig. 1H, Table 2).

NFPs regulate ventricular trabeculation in a cardiomyocyte-autonomous manner

We then examined the formation of trabeculae, which are sheet-like structures extending from the compact zone, in control and MDKO hearts. E10.5 *MDKO; mTmG* and *Nkx2.5*$^{Cre/+}$*; mTmG* embryos, in which Nkx2.5-expressing cells were GFP positive, were stained for PECAM (Pecam1) to identify endocardial/endothelial cells. When whole hearts were three-dimensionally (3D) imaged by confocal microscopy we found that control trabecula had a diameter of one or two cells, whereas the MDKO trabecula had a diameter of two or three cells at E10.5 (Fig. 2A,B; supplementary material Movie 2, Fig. S3). The number of trabeculae and the thickness of the trabeculae and the compact zone were quantified. Beginning at E10.5, MDKO hearts displayed fewer trabeculae per unit length but thicker trabeculae compared with controls (Fig. 2C-E). The thickness of the compact zone was not significantly different between control and MDKO from E10.5 to E13.5, whereas at E14.5 the compact zone of MDKO was thinner than that of the control (Fig. 2C-E), indicating a non-compaction defect, consistent with a previous report (Yang et al., 2012). Dual-fluorescence staining of heart sections with MF20 (which recognizes myosin II heavy chain) and PECAM antibodies (Chen et al., 2009) showed that endocardial cells could invade the cardiac jelly and surround the myocardium in both MDKO and control (Fig. 2A-D), indicating that the trabeculation defect was not due to a defect in endocardial cell invasion.

The variety of defects in the MDKO might be caused by the loss of NFP function in different cardiac cell types. To determine the population that is responsible for these morphogenetic defects, *SM22-Cre*, *Tie2-Cre*, *Wnt1-Cre*, *WT1*^{CreERT2} and *Mef2c-Cre* were applied to delete NFPs in cardiomyocytes, endothelial cells, CNCCs, epicardial cells and cells derived from the SHF, respectively. The deletion of NFPs in cardiomyocytes via *SM22-Cre*, which is expressed in cardiomyocytes at the early stage of heart development in addition to its expression in smooth muscle cells (Li et al., 1996; Umans et al., 2007; Stankunas et al., 2008), resulted in trabeculation defects with thicker trabeculae and a decreased number of trabeculae per unit length at E14.5 (supplementary material Fig. S2A,B), whereas NFP deletion mediated by *Tie2-Cre*, *Wnt1-Cre* or *WT1*^{CreERT2} did not display any trabeculation defects (supplementary material Fig. S2A-D; data not shown), indicating that NFPs regulate trabeculation in a cardiomyocyte-autonomous manner.

NFPs in the SHF are required for OFT and atrioventricular septation

We further determined that NFP deletion mediated by *SM22-Cre*, *Tie2-Cre* and *WT1*^{CreERT2} in cardiomyocytes, endocardial/endothelial cells and epicardial cells, respectively, did not display any defects in morphogenesis (supplementary material Fig. S2A; data not shown), indicating that the function of NFPs in differentiated cardiomyocytes, endocardial cells or epicardial cells does not contribute to cardiac morphogenesis. *Wnt1-Cre*-mediated NFP deletion in CNCCs caused cranial facial defects (supplementary material Fig. S2C), but no obvious cardiac morphogenesis defect (supplementary material Fig. S2D), indicating that NFP function in

Table 2. MDKO morphogenetic defects at E13.5 and 14.5

Age	Trabeculation defect	Valvular defect	AVSD	PTA	DORV
E13.5	17/17	17/17	17/17	2/12	17/17
E14.5	8/8	8/8	8/8	0/8	8/8

Nkx2.5-Cre$^{+/-}$*; Numb*$^{fl/+}$*; Numbl*$^{fl/fl}$ or *Nkx2.5-Cre*$^{+/-}$*; Numb*$^{fl/fl}$*; Numbl*$^{fl/+}$ males were crossed to *Numb*$^{fl/fl}$*; Numbl*$^{fl/fl}$ females to generate the MDKO. Shown in each case is: total number of mutants that displayed the defect/total number of mutants that were examined.
AVSD, atrioventricular septal defect; PTA, persistent truncus arteriosus; DORV, double outlet right ventricle.

Development (2014) doi:10.1242/dev.093690

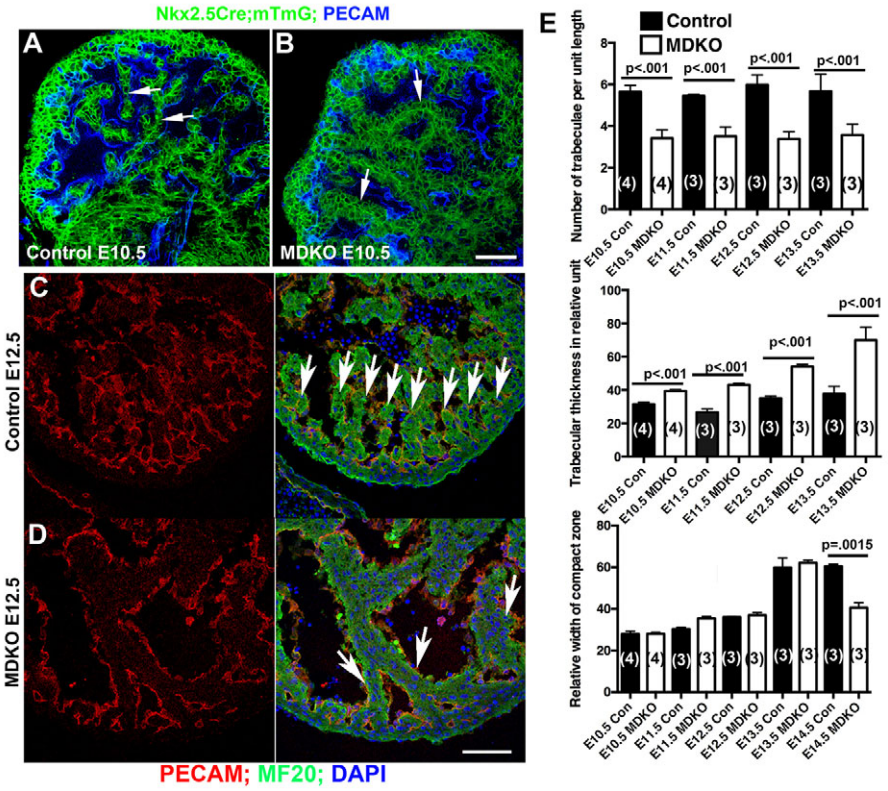

Fig. 2. NFPs are required for myocardial trabeculation. (A,B) E10.5 *Nkx2.5*$^{Cre/+}$*; mTmG* and *MDKO; mTmG* whole hearts were stained for PECAM and then 3D imaged. The control trabecula has a diameter of one or two cells, whereas the MDKO trabecula has a diameter of two or three cells (trabeculae indicated by arrows). Images are one section from *z*-stacks (the whole 130 µm stacks are shown in supplementary material Movies 2, 3). (C,D) Control and MDKO hearts were stained with MF20 and PECAM antibodies. Endocardial cells in MDKOs can invade the cardiac jelly and contact cardiomyocytes. The control heart displayed more trabeculae per unit length than the MDKO. Arrows indicate the trabeculae. (E) Quantification of trabeculae density, trabeculae thickness and compact zone thickness. The MDKO hearts had fewer trabeculae per unit length, but the trabeculae were thicker than those of the control hearts. Error bars indicate s.d.; *n* values are shown within each bar. Scale bars: 100 µm.

CNCCs does not contribute to cardiac morphogenesis. Instead, *Mef2c-Cre*-mediated deletion in the SHF recapitulated the OFT septation defect and alignment defect in six out of ten E13.5 mutant hearts (supplementary material Fig. S2E), AVSD in eight out of ten mutant hearts (Fig. 3A) and trabeculation defect in the right ventricle in four out of four mutant hearts (data not shown). *Mef2c-Cre* is not active in the endocardial cells of the atrioventricular cushion (AVC) (Fig. 3B), indicating that the AVSD is not caused by the lack of NFPs in endocardial cells of the AVC, which is consistent with the observation that *Tie2-Cre*-mediated NFP deletion did not cause any defects.

Both *Nkx2.5*$^{Cre/+}$-mediated and *Mef2c-Cre*-mediated mutants lacked the DMP (Fig. 1H, Fig. 3A), which is required for atrioventricular septation (Snarr et al., 2007b; Hoffmann et al., 2009). Using lineage tracing and 3D imaging, we observed that cells derived from the SHF migrated to the AVC and formed the DMP in the control, but fewer (data not shown) or no cells (Fig. 3C,D; supplementary material Movies 4, 5) were observed in the DMP in the knockout, indicating that NFPs are required for the migration of cells in the posterior SHF to form the DMP and the atrioventricular septum. In control hearts, *Mef2c-Cre*-labeled cardiomyocytes displayed myocardial spikes protruding towards the cushion in the OFT region (Fig. 3E), indicating a polarized migration toward the cushion. In the mutants, most of the NFP-null cells lacked myocardial spikes and fewer cells invaded the OFT cushion (Fig. 3E).

MDKOs display differentiation defects

Whole-mount *in situ* hybridization of E9.5-12.5 embryos with probes of the heart chamber markers *ANP* (*Nppa* – Mouse Genome Informatics) and *Hand1* demonstrated that their expression patterns in the ventricles did not differ between control and MDKO hearts (supplementary material Fig. S3A), indicating that there are no chamber specification defects. We then screened for genome-wide transcriptional differences between control and MDKO E10.5 ventricles via mRNA deep sequencing (supplementary material Table S1). There were 340 genes with an expression ratio of MDKO to control that was higher than 1.7 (P<0.05) and 474 genes with a ratio of MDKO to control that was lower than 0.6 (P<0.05) (supplementary material Table S2). Of the 814 dysregulated genes, 42 have been reported to be involved in heart morphogenesis and heart diseases (Fig. 4A). Notably, genes that are involved in the differentiation of progenitors in the SHF, such as *Isl1*, *Shox2*, *Fgf8*, *Hoxa3* and *Tbx1*, were expressed at significantly higher levels in MDKO than in control (Fig. 4A). The transcriptional differences were consistent with the Q-PCR results (Fig. 4B). The expression of *Isl1* (Cai et al., 2003) was consistently upregulated 2- to 4-fold in E9.5-11.5 MDKO hearts (Fig. 4C). The transcription of *Isl1* in OFT, where the Isl1-expressing cells accumulate, was ~30-fold higher than in the ventricles (Fig. 4D). *Isl1* expression in the OFT of the MDKO is about double that in the OFT of the control, similar to its upregulation in the ventricles (Fig. 4D). *Isl1* transcription, as assessed by *in situ* hybridization, did not show any obvious expansion from right to left ventricle in the MDKO (data not shown). Instead, we observed more *Isl1*-expressing cells in the OFT of the MDKO based on IF staining (Fig. 4E).

Cardiomyocyte differentiation is a sequential process and to further define the differentiation defect we examined the expression of genes that encode cardiac differentiation regulators and structural proteins in E12.5 and E13.5 hearts by Q-PCR. *Irx3*, *Irx4*, *Irx5* and *Myh6* were significantly downregulated in the MDKO, whereas *Myh11* and *Bmp10* were upregulated and *Myh7*, *Myl2* and *Tnnt2* were not significantly different from the control (Fig. 4F). The ratio of Mhc7:Mhc6 after being normalized to cyclophilin A (peptidylprolyl isomerase A) was ~2-fold greater in the MDKO than in the control at both E12.5 and E13.5, indicating a cardiomyocyte differentiation defect. Transcriptional patterns of *Irx3* and *Irx4* were investigated by *in situ* hybridization. *Irx3* was uniformly expressed

Development (2014) doi:10.1242/dev.093690

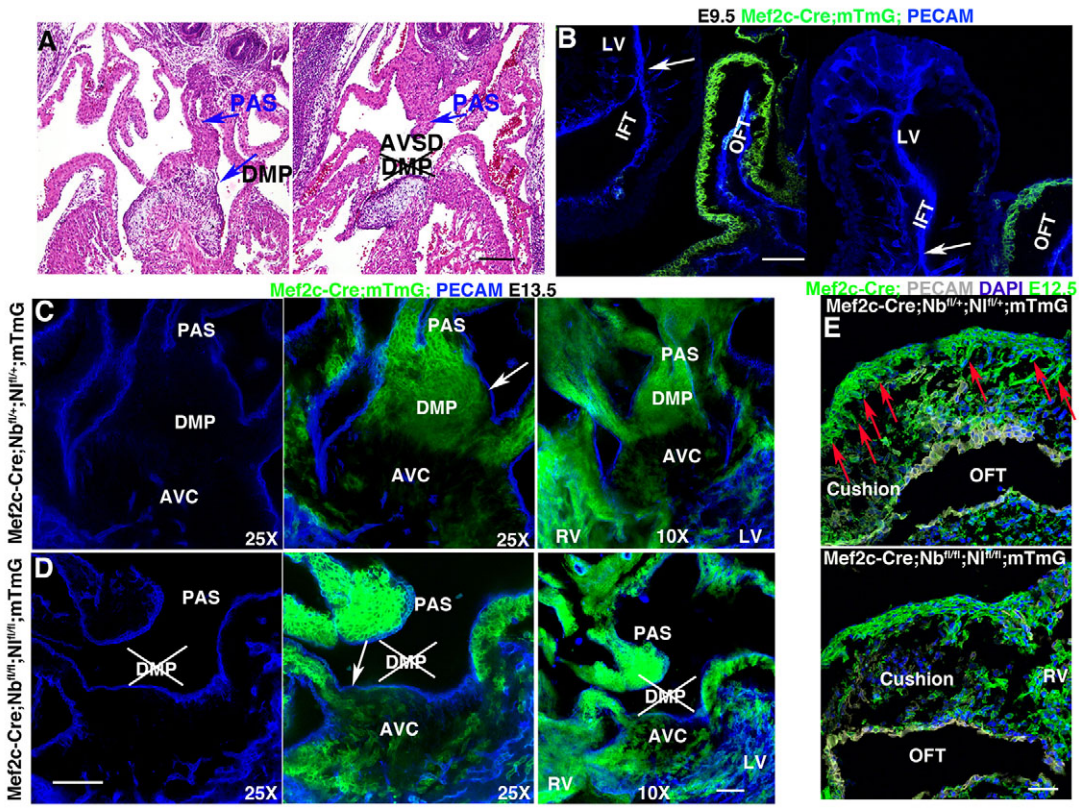

Fig. 3. NFPs in the SHF are required for dorsal mesenchymal protrusion development and atrioventricular septation. (A) *Mef2c-Cre*-mediated NFP knockout displayed absence of the dorsal mesenchymal protrusion (DMP) (arrows). (B) *Mef2c-Cre* is active in endocardial cells of the OFT but not AVC of the inflow tract (IFT) and left ventricle (LV) region. Arrows indicate IFT. (C,D) Lineage tracing indicated that cells from the SHF contribute to the DMP in the control, whereas in the knockout *Mef2c-Cre*-labeled cells do not migrate to the AVC to form the DMP. Arrows indicate endocardial cells of the AVC. One section from a 3D imaged *z*-stack is shown in C and D (for whole stacks see supplementary material Movies 4, 5). The lower magnifications (10×) are shown to indicate their orientation (which can also be determined from A). PAS, primary atria septum. (E) Mef2c-Cre-labeled control cells form myocardial spikes that are oriented perpendicular to the wall (red arrows indicate the spikes), whereas NFP-null cells do not show spike formation. Scale bars: 100 µm.

in the trabeculae of the control heart, whereas the MDKO pattern was less uniform and there was no *Irx3* expression in some trabeculae (Fig. 4G). *Irx4*, which specifies cardiomyocytes in ventricles (Bao et al., 1999; Bruneau et al., 2001), was expressed in the compact and trabecular zones in controls, whereas in MDKOs the compact zone exhibited weaker or no expression of *Irx4* (Fig. 4G). We found that 88% of the trabeculae in the control displayed organized sarcomere arrays at E12.5 (n=4 hearts), whereas in the MDKO only 15% of the trabeculae displayed sarcomeric arrays (n=3 hearts) (Fig. 4H). In summary, MDKO hearts displayed defects in the differentiation of cardiac progenitors and in the maturation of sarcomeres.

Numb regulates cardiac progenitor differentiation through its function in endocytosis

Cardiomyocyte differentiation in cultured mouse embryoid bodies (EBs) recapitulates the genetic network that regulates this process *in vivo* (Smith, 2001; Mummery et al., 2002). To study NFP regulation of cardiac progenitor differentiation, we took advantage of a pluripotent P19 embryonal carcinoma cell line (P19Cl6-GFP) (McBurney and Rogers, 1982; Habara-Ohkubo, 1996), in which *GFP* is under the transcriptional control of the rat *Mlc-2v* promoter and therefore functions as a marker for differentiated cardiomyocytes (Moore et al., 2004). Adenovirus-mediated expression of Numb (p65 isoform) in the EB increased the number of GFP^+ cells (Fig. 5A-C) and the number of beating cultures (data not shown), suggesting that Numb overexpression promotes cardiomyocyte differentiation. We examined the expression of genes that are involved in cardiac progenitor differentiation and those that encode structural proteins. *Nkx2.5*, *Gata6*, *ANP*, *Irx3*, *Myh7* and *Myh6* were all upregulated 2- to 4-fold (Fig. 5D), whereas progenitor cell markers *Isl1* and *Gata4* were significantly downregulated (Fig. 5D).

Numb interacts with endocytic adapters such as α-adaptin and Eps15 via the NPF and DPF motifs in the C-terminus (Salcini et al., 1997; Santolini et al., 2000) to selectively promote clathrin-dependent endocytosis of transmembrane proteins including Notch1 and the EGF receptor (Traub, 2003; Sorkin, 2004). To determine if Numb regulates cardiomyocyte differentiation via endocytosis, EB cultures were treated with Bafilomycin A1 (BafA1), an inhibitor of endocytosis. BafA1 abolished the Numb-induced increase in cardiac progenitor differentiation (Fig. 5E). When the α-adaptin or Eps15 binding sites (NPF and DPF, respectively) of Numb were mutated to generate $NbNPF^m$ and $NbDPF^m$ they failed to promote differentiation, as evidenced by fewer GFP^+ cells and no upregulation of *Nkx2.5*, *Gata6* and *Myh7* (Fig. 5F,G). We then examined whether Numb can normalize Isl1 expression in E9.5 MDKO hearts using an *ex vivo* culture system. Ad-Numb, but not Ad-$NbDPF^m$, reduced *Isl1*, *Fgf8* and *Shox2* expression significantly in the MDKO (Fig. 5H). These results demonstrate that NFPs

Development (2014) doi:10.1242/dev.093690

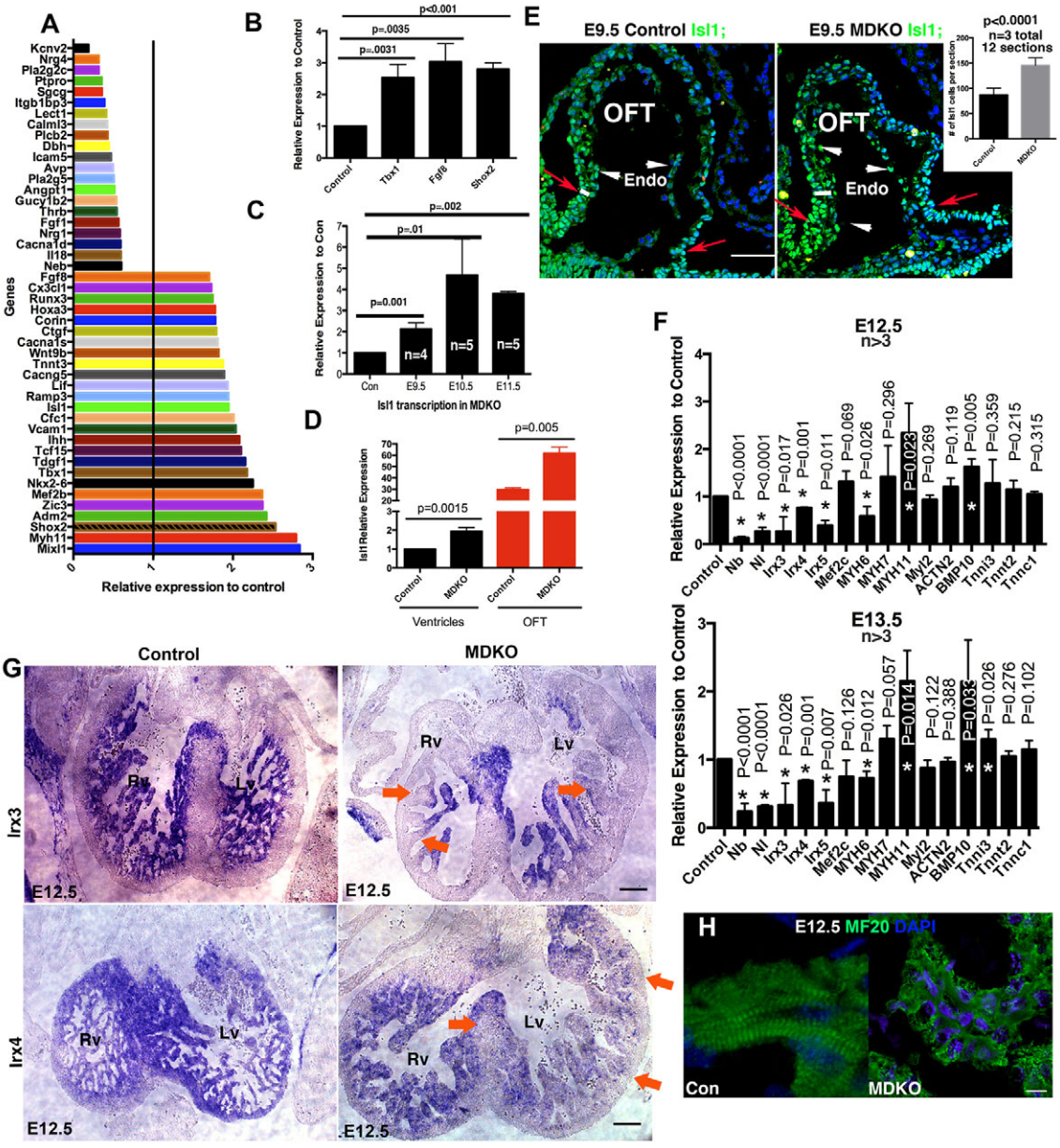

Fig. 4. MDKOs display cardiomyocyte differentiation and maturation defects. (A) mRNA deep sequencing showed that multiple genes involved in cardiac morphogenesis and disease are dysregulated in the MDKO. (B) Q-PCR showing the upregulation of *Tbx1*, *Fgf8* and *Shox2*. (C) Transcription of *Isl1* was upregulated in the MDKO ventricles from E9.5 to E11.5 as compared with controls based on Q-PCR. (D) Compared with control, *Isl1* expression in the OFT of the MDKO increased to a similar extent as in the ventricles. (E) There are two or three layers of Isl1 protein-positive cells in the control OFT, whereas there are three or four layers in MDKO OFT (red arrows and white bars). White arrows indicate endocardial cells. The inset shows quantification of $Isl1^{+}$ cells in control and MDKO hearts, with four sections for each heart and a total of three hearts. (F) Cardiomyocytes in E12.5 and E13.5 MDKO hearts displayed differentiation defects, with significantly lower expression of *Irx3*, *Irx4*, *Irx5* and *Myh6* but higher expression of *Bmp10* and *Myh11*. (G) The trabecular cardiomyocyte specification gene *Irx3* was not expressed in some trabeculae, and the ventricular cardiomyocyte specification gene *Irx4* was not transcribed in some regions based on *in situ* hybridization. The arrows indicate zones that did not transcribe *Irx3* or *Irx4*. (H) MF20 staining demonstrated that the MDKO displayed a sarcomere array formation defect. Error bars indicate s.d. Asterisks indicate statistical significance at $P \leq 0.05$. Scale bars: 100 µm in E,G; 10 µm in H.

regulate cardiac progenitor differentiation in an endocytosis-dependent manner.

Both CBF1-dependent and -independent Notch signaling are upregulated in MDKO hearts

Numb negatively regulates Notch1 signaling, and the MDKO phenotype is comparable to that of transgenic mice expressing activated Notch1 in cardiogenic mesoderm (Watanabe et al., 2006), which led us to investigate Notch1 signaling in MDKO hearts. We examined the level of Notch1 intracellular domain (NICD1), the activated form of the Notch1 receptor, in control and MDKO hearts. MDKO hearts displayed higher levels of NICD1 protein (Fig. 6A). IF staining showed that endocardial cells were positive for NICD1 (Fig. 6B; supplementary material Fig. S4A), consistent with a previous report (Grego-Bessa et al., 2007), whereas in MDKOs NICD1 staining was also observed in some cardiomyocyte nuclei at

Development (2014) doi:10.1242/dev.093690

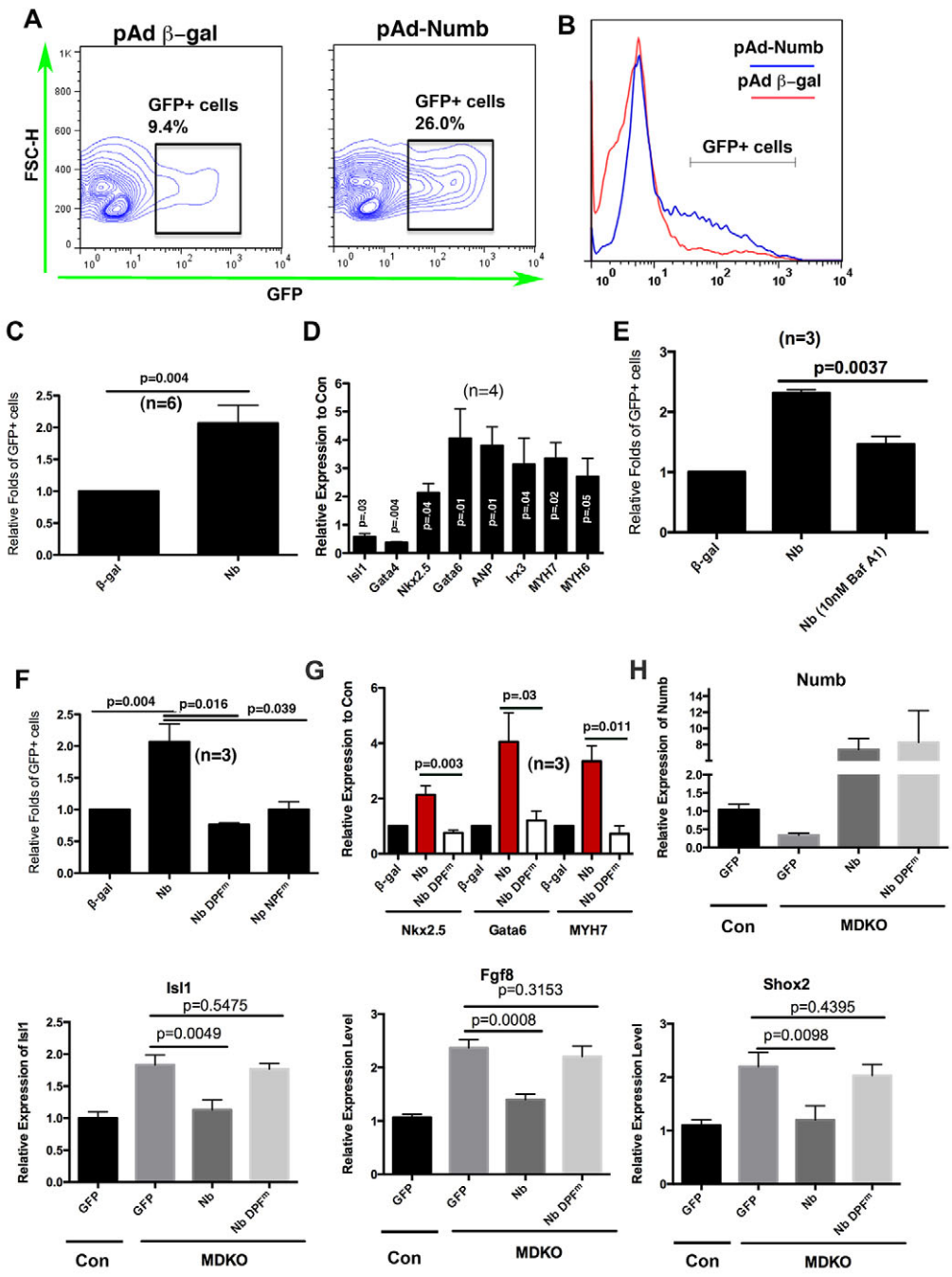

Fig. 5. Numb regulates cardiac progenitor differentiation via endocytosis. (A-C) Numb overexpression in EB culture promotes the differentiation of P19Cl-6GFP cells, in which GFP is under the control of rat *Mlc-2v*, as evidenced by increased numbers of GFP$^+$ cells compared with β-gal-overexpression EB cultures. The percentage of GFP$^+$ cells was quantified by flow cytometry. FSC, forward scatter channel. (D) Numb overexpression EB cultures showed higher expression of *Nkx2.5*, *Gata6*, *ANP* (*Nppa*), *Irx3*, *Myh7* and *Myh6*, but lower expression of *Isl1* and *Gata4*. (E) The endocytosis inhibitor BafA1 abolished Numb overexpression-induced EB culture differentiation. (F,G) Endocytosis-defective Numb variants: both NbDPF^m and NbNPF^m failed to enhance cardiomyocyte differentiation and induce *Nkx2.5*, *Gata6* and *Myh7* expression using the EB culture system. (H) Using an *ex vivo* culture system, Numb, but not NbDPF^m and control virus GFP, could rescue the expression of *Isl1*, *Fgf8* and *Shox2* in E9.5 MDKO hearts. *Isl1* and *Numb* expression in the control and virus-infected MDKO hearts was examined by Q-PCR. *Isl1* expression in GFP-infected wild-type hearts was set as 1. Error bars indicate s.d.

E9.5 (Fig. 6B) and in all nuclei at E12.5 (supplementary material Fig. S4A).

To determine whether upregulation of Notch signaling in MDKO hearts is dependent on CBF1/canonical Notch signaling, the transgenic Notch reporter (TNR) line (Duncan et al., 2005), in which GFP expression is under the control of CBF1 (Rbpj – Mouse Genome Informatics), a downstream target of Notch signaling, was used to generate the *MDKO; TNR* strain. GFP intensity was stronger in *MDKO; TNR* hearts than in the control (supplementary material Fig. S4B). Western blot indicated that GFP levels were higher in eight out of nine *MDKO; TNR* hearts than in littermate controls (Fig. 6C), indicating upregulated canonical Notch signaling in MDKO hearts. We observed GFP in some cardiomyocytes as well as endocardial cells in *MDKO; TNR* hearts at E9.5 (Fig. 6D). However, at E12.5, although all cardiomyocytes expressed NICD1 (supplementary material Fig. S4A), not all of them were TNR/GFP$^+$ (supplementary material Fig. S4C). The discrepancy is due to TNR incompletely representing all NICD1$^+$ cells, indicating that NFPs regulate both canonical and non-canonical – or CBF1-dependent and -independent – Notch signaling (Hellström et al., 2007; Mizutani et al., 2007; Sanalkumar et al., 2010).

Expression levels of Notch target genes, including *Hey1*, *Hey2*, *Heyl* and *Hes1*, were used to assess the activation of Notch signaling in MDKO hearts. Q-PCR showed that *Hey1* and *Hes1* expression levels were slightly higher in MDKO hearts than controls at certain ages (supplementary material Fig. S4D). To confirm that Notch signaling was upregulated in NFP-null cardiomyocytes, we used a lentivirus RBP-Jk luciferase reporter

Development (2014) doi:10.1242/dev.093690

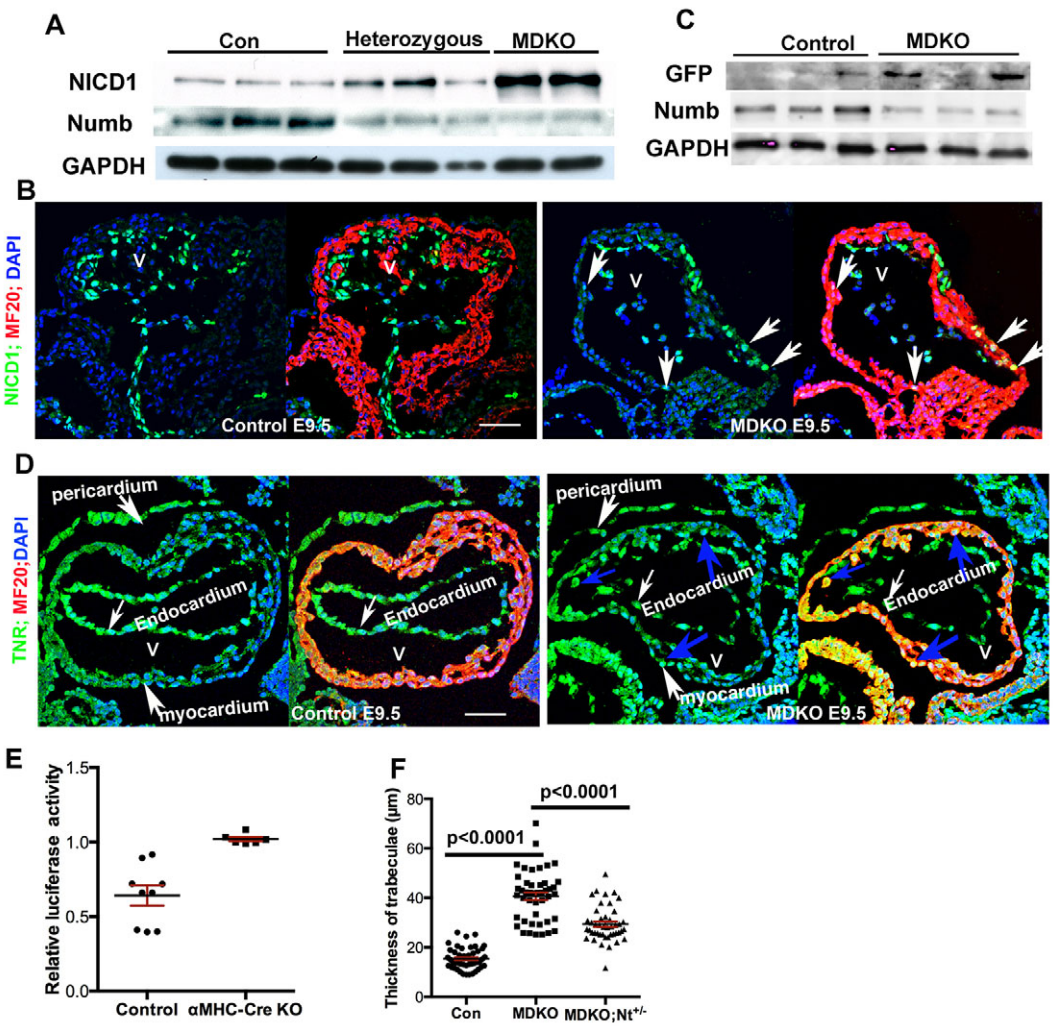

Fig. 6. MDKO hearts display elevated Notch signaling. (A) E12.5 ventricles were lysed for NICD1 western blot. MDKO and heterozygous hearts showed higher levels of NICD1 protein than controls. (B) IF showed that some cardiomyocytes in E9.5 MDKO but not control hearts were NICD1 positive (white arrows). (C) E12.5 ventricles were lysed for GFP quantification and eight out of nine *MDKO; TNR* hearts displayed higher levels of GFP protein than the control. (D) GFP staining in sections from E9.5 TNR control and *MDKO; TNR* hearts showed that Notch signaling is active in endocardial cells in the control, whereas in the MDKO some cardiomyocytes are also positive (blue arrows). (E) Lenti RBP-Jk luciferase reporter assay showed that cardiomyocytes from *αMHC-Cre*-mediated NFP knockout hearts displayed higher Notch signaling activation than the control. (F) The thickness of trabeculae of *MDKO; Nt*$^{fl/+}$ hearts was significantly decreased compared with that of MDKO. The incomplete Numb deletion in MDKO in A and C was due to its expression in epicardial and endocardial cells. V, ventricle. Scale bars: 50 μm.

to measure Notch signaling activation in cardiomyocytes that were isolated from control or *αMHC-Cre*-mediated cardiomyocyte-specific NFP knockout hearts. The NFP knockout showed higher Notch signaling activation, indicating upregulated Notch signaling in cardiomyocytes (Fig. 6E).

To determine whether upregulated Notch1 signaling was responsible for the defects in morphogenesis in MDKO hearts, Notch1 signaling was suppressed by deleting one of the *Notch1* alleles (Garg et al., 2005) in the MDKO to generate *MDKO; Nt*$^{fl/+}$. This resulted in reduced NICD1 staining intensity (supplementary material Fig. S4A). However, this reduction did not rescue the OFT septation defect or AVSD (data not shown). Instead, Notch1 suppression did reduce the thickness of the trabeculae, although it did not increase the number of trabeculae per unit length (Fig. 6F; supplementary material Fig. S5A,B). This suggests that NFPs regulate trabecular thickness through Notch1 signaling.

NFPs regulate cardiomyocyte proliferation through inhibition of Notch1 signaling

To examine if the thicker trabeculae and the larger size of MDKO hearts are due to an increase in cell proliferation, the cardiomyocyte proliferation rate was assessed by BrdU pulse labeling (Fig. 7A,B). In the compact zone, the percentage of BrdU-positive cardiomyocytes in the MDKO was significantly higher than in the control from E9.5 to E12.5 (Fig. 7C), consistent with the increased heart size in MDKOs. This result was also apparent specifically in the trabecular zone, where there was a 3-fold increase in the percentage of BrdU-positive cells in the MDKO compared with the control at E12.5 (Fig. 7D), consistent with the thicker trabeculae in MDKOs.

We examined the mRNA deep sequencing data and found, among the known cell cycle regulators, that only *p57* (*Cdkn1c* or *p57*^{kip2}), a cyclin-dependent kinase inhibitor, was significantly different. Expression levels of cyclin D1 (*Ccnd1*), *Cdkn1a* (*p21*) and *p57* were further examined by Q-PCR and only *p57* was significantly different from the control in E9.5-13.5 MDKO hearts (Fig. 7E). We then examined whether reduced *p57* expression in MDKOs was caused by increased Notch1 signaling. *MDKO; Nt*$^{+/fl}$ mice showed increased *p57* expression compared with the MDKO (Fig. 7F). Consistent with the higher expression of p57 and the thinner trabeculae, cardiomyocyte proliferation in the trabeculae of *MDKO; Nt*$^{+/fl}$ mice was significantly reduced compared with the MDKO (Fig. 7G). To further study how NFPs regulate *p57*, embryonic cardiomyocytes from control, *Numb*$^{flox/flox}$; *Numbl*$^{flox/flox}$ or *Notch1*$^{flox/flox}$; *Numb*$^{flox/flox}$; *Numbl*$^{flox/flox}$ were cultured and treated with Ade-Cre to induce recombination. We found that *p57* was downregulated in *Cre*$^{+}$; *Numb*$^{flox/flox}$; *Numbl*$^{flox/flox}$ cardiomyocytes, but was upregulated in *Cre*$^{+}$; *Notch1*$^{flox/flox}$; *Numb*$^{flox/flox}$; *Numbl*$^{flox/flox}$ cardiomyocytes (Fig. 7H,I), indicating that downregulation of *p57* in NFP-null cardiomyocytes is Notch1 dependent.

Development (2014) doi:10.1242/dev.093690

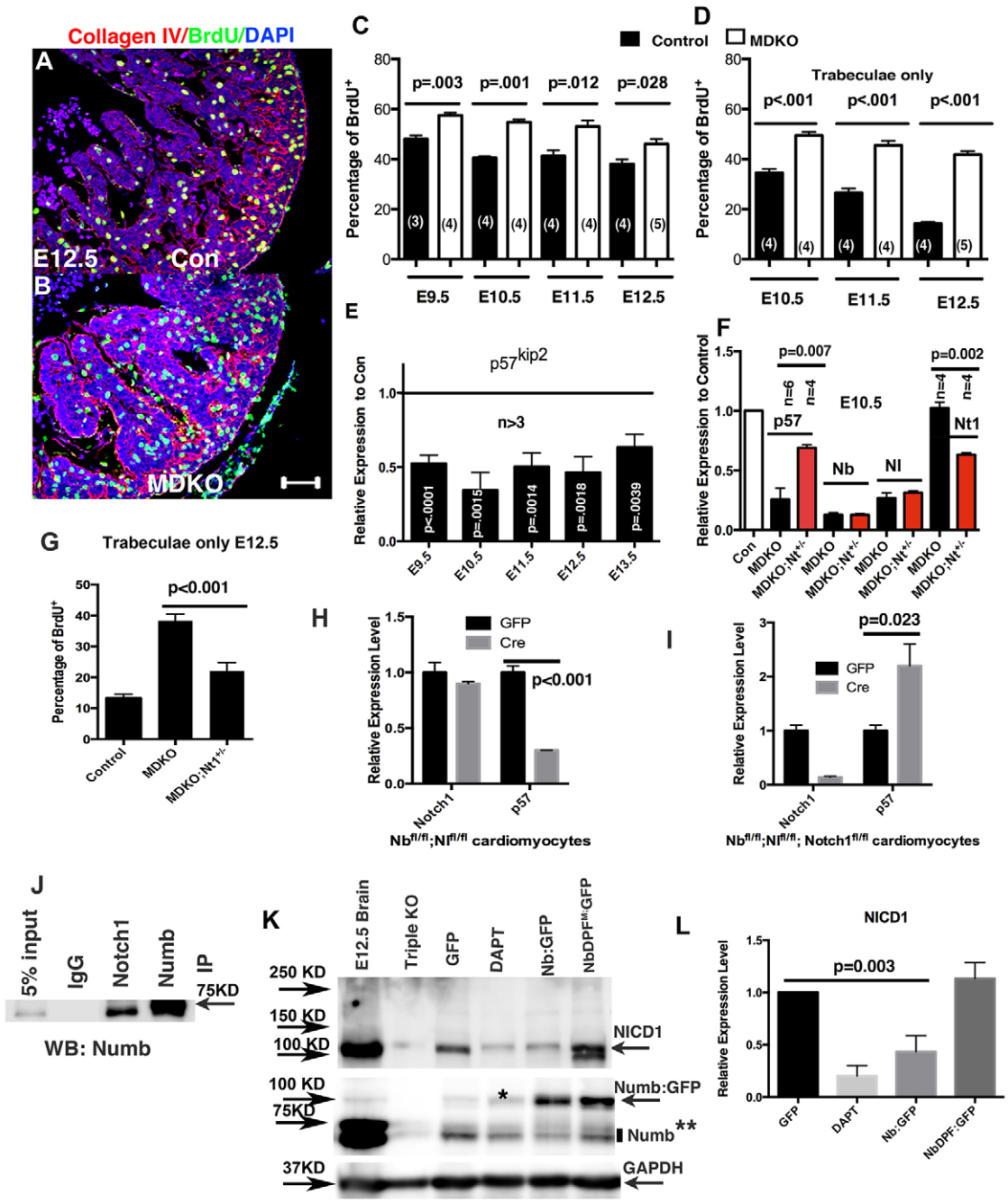

Fig. 7. NFPs regulate cardiomyocytes proliferation via Notch1. (A,B) BrdU pulse labeling indicated that cardiomyocytes in the MDKO proliferated at a higher rate than those in the control. Cardiomyocytes were identified by collagen IV, a marker for the basement membrane. (C,D) MDKO displayed higher proliferation rates of cardiomyocytes in the compact zone (C) and in the trabecular zone (D) at various ages. (E) Transcription of the cell cycle inhibitor *p57* (*p57*^{kip2}) was significantly reduced in the MDKO. (F) *p57* expression was partially rescued in *MDKO; Nt*$^{fl/+}$. The expression of *Numb* (Nb), *Numbl* (Nl) and *Notch1* (Nt1) in *MDKO; Nt*$^{fl/+}$ was comparable to their expression in MDKO. (G) Trabecular cardiomyocyte proliferation was reduced in E12.5 *MDKO; Nt1*$^{+/fl}$ compared with the control. (H,I) *p57* expression was downregulated in *Nb*$^{fl/fl}$*; Nl*$^{fl/fl}$ cardiomyocytes but upregulated in *Nb*$^{fl/fl}$*; Nl*$^{fl/fl}$*; Notch1*$^{fl/fl}$ after Cre-mediated recombination for 72 hours. (J) Numb and Notch1 antibody can immunoprecipitate Numb using P4 heart lysates. IP, immunoprecipitate; WB, western blot. (K) DAPT inhibited Notch1 cleavage to produce NICD1, and overexpressing Numb:GFP but not NbDPF^{m}:GFP reduced NICD1 in cultured embryonic cardiomyocytes. E12.5 mouse brain and *Nb*$^{fl/fl}$*; Nl*$^{fl/fl}$*; Notch1*$^{fl/fl}$ cardiomyocytes treated with pAd-Cre were used as positive and negative control, respectively. *A weak band in the positive control, DAPT and GFP lanes that is non-specific. **The Numb antibody can detect all four Numb isoforms. (L) Quantification of NICD1 in different treatments from three independent experiments. Error bars indicate s.d. Scale bar: 50 µm.

To study how NFPs regulate Notch1 signaling, we first determined whether Notch1 and Numb interact in the heart. Both Numb and Notch1 antibodies could pull down Numb based on co-immunoprecipitation using whole heart lysates (Fig. 7J) or endocardial cell-specific NFP-null heart lysate (Wu et al., 2012) (supplementary material Fig. S6A), indicating that Numb interacts with Notch1 in the mouse heart. To determine how Numb inhibits Notch1 signaling, Numb was overexpressed in cultured embryonic

Development (2014) doi:10.1242/dev.093690

cardiomyocytes. Western blot indicated that Numb:GFP overexpression reduced the level of NICD1. However, overexpressing GFP or the endocytosis-defective NbDPF^{m}:GFP did not reduce the level of NICD1 (Fig. 7K,L), indicating that Numb promotes NICD1 degradation via endocytosis.

DISCUSSION

NFPs play multiple roles during cardiac development and their disruption results in multiple CHDs

The defects in trabeculation, proliferation, progenitor differentiation, OFT and atrioventricular septation and OFT alignment in MDKO hearts, together with the recent report that NFPs inhibit Notch2 to regulate compaction (Yang et al., 2012), demonstrate that NFPs are essential for cardiac development and morphogenesis. These findings extend our previous analysis which found that NFPs are essential for epicardial development (Wu et al., 2010). Our present analysis using NFP knockout models mediated by *Tie2-Cre*, *Wnt1-Cre*, *SM22-Cre*, *WT1^{CreERT2}*, *Mef2c-Cre* and *Nkx2.5$^{Cre/+}$* suggests that the key functions of NFPs in cardiac development are stage- and cell type-specific. NFP knockouts mediated by *Tie2-Cre*, *WT1^{CreERT2}* and *Wnt1-Cre* did not display any obvious cardiac morphogenetic defects (supplementary material Fig. S2), indicating that NFP functions in endocardial cells, epicardial cells and CNCCs are not essential for heart morphogenesis. *SM22-Cre*-mediated NFP knockout in cardiomyocytes partially phenocopied the MDKO, with disrupted trabeculation, but did not display differentiation and morphogenetic defects (supplementary material Fig. S2). *Mef2c-Cre*-mediated NFP knockouts recapitulated the morphogenesis defects of the MDKO, indicating that NFPs in the SHF are essential for cardiac morphogenesis (Fig. 3; supplementary material Fig. S2). The difference in phenotypes between *SM22-Cre*-mediated and *Nkx2.5$^{Cre/+}$*-mediated mutants might be due to the different timing and cell types in which NFPs were deleted. *Nkx2.5$^{Cre/+}$* was active in cardiomyocytes derived from the FHF and SHF, some endocardial cells of the OFT and AVC (supplementary material Fig. S1A,B), and very few endocardial cells of the ventricles (supplementary material Fig. S1C, Movie 1) and was active beginning at E7.5 based on *Nkx2.5$^{Cre/+}$; mTmG*. By contrast, *SM22-Cre* is active in some cardiomyocytes in the E8.5 heart tube, but not in all cardiomyocytes until ~E9.0, a stage at which cardiac progenitor cells have already initiated the differentiation process.

However, the expression of *Nkx2.5$^{Cre/+}$* in the endocardial cells appears not to be the cause of the AVSD and OFT septation in the MDKO, as *Tie2-Cre*-mediated NFP deletion did not cause any defect. Furthermore, NFP deletion via *Mef2c-Cre*, which is not active in the endocardial cells of the AVC (Fig. 3B), caused the AVSD, indicating that NFP absence in endocardial cells of the AVC is not responsible for the AVSD in the mutants. Instead, the morphogenesis defects in MDKOs might be caused by the SHF progenitor cell differentiation defect, as evidenced by the upregulation of *Isl1*, *Fgf8*, *Hoxa3* and *Tbx1* in MDKOs. This is consistent with previous reports that down- or upregulation of *Fgf8/Fgf10* (Kelly et al., 2001; Ilagan et al., 2006; Park et al., 2006), *Isl1* (Ai et al., 2007; Kwon et al., 2007; Lin et al., 2007; Ueno et al., 2007) and *Tbx1* (Vitelli et al., 2002) interferes with SHF progenitor cell differentiation and subsequently causes cardiac morphogenetic defects or CHDs (Buckingham et al., 2005; Black, 2007; Rochais et al., 2009). Further studies showed that NFP-null cells fail to form myocardial spikes that orient perpendicularly to the heart wall (Fig. 3E) and fail to migrate into the OFT cushion, which might result in the OFT septation defect.

NFPs regulate ventricular trabeculation and compaction

Ventricular trabeculation and compaction are two related but different biological processes during cardiac morphogenesis. Trabeculation initiates at E9.0-9.5 and myocardial compaction occurs at ~E14.5 (Samsa et al., 2013; Zhang et al., 2013). Lack of trabeculation causes embryonic lethality in mice and excess trabeculation causes cardiomyopathy and heart failure in humans (Jenni et al., 1999; Weiford et al., 2004; Breckenridge et al., 2007). Despite the fundamental nature of these morphogenic processes, the molecular and cellular mechanisms controlling trabeculation and compaction are not fully understood. Pathways that regulate trabeculation include the Notch1 and Notch2 signaling pathways. Global or endothelial-specific *Notch1* deletion causes ventricular hypoplasia and trabeculation defects (Grego-Bessa et al., 2007). Notch1 activation in early cardiac cell lineages by *Mesp1-Cre*-mediated overexpression of NICD1 leads to several cardiac morphogenetic defects, including abnormal ventricular morphology similar to ventricular non-compaction (Watanabe et al., 2006). However, NICD1 overexpression in cardiomyocytes at a later stage via *Mlc-2v-Cre* does not cause obvious trabecular morphogenesis (Croquelois et al., 2008). The discrepancy could be caused by Notch1 activation at different developmental stages or in different cell populations.

Notch2 intracellular domain (N2ICD) is detected throughout the myocardium before E11.5, but at a later stage Notch2 activity is specifically downregulated in the compact zone and is restricted in trabecular myocardium during ventricular compaction (Yang et al., 2012). *Notch2* global knockout displays ventricular hypoplasia (McCright et al., 2001). *Notch2* deletion in heart via *SM22-Cre* displays cyanosis at birth due to narrow arteries, but whether or not the knockout displays a trabeculation defect was not reported (Varadkar et al., 2008). However, loss-of-function analysis for Notch1 or Notch2 in cardiomyocytes cannot determine whether they are involved in trabecular morphogenesis, as all four Notch receptors are expressed at relatively high levels in the heart (supplementary material Fig. S6B) and the deletion of one Notch receptor in cardiomyocytes may be compensated by the function of another, although they might not be expressed in cardiomyocytes under normal conditions. Yang et al. (Yang et al., 2012) reported that N2ICD continues to be present in the compact zone at E12.5 and E13.5, which was not observed in the control, and we observed that NICD1 is present in cardiomyocytes in both the compact and trabecular zones of the MDKO, indicating that NFPs regulate trabecular morphogenesis via inhibition of both Notch1 and Notch2.

Trabecular morphogenesis is a multistep process that includes, but is not limited to, trabecular initiation, proliferation/growth, differentiation and compaction. Notch1 and Notch2 might regulate different steps of trabecular morphogenesis. Genetic epistasis studies can determine whether Notch receptors function downstream of NFPs in the regulation of a particular trabecular morphogenesis step. MDKOs displayed lower *p57* expression, higher proliferation rates and thicker trabeculae. When one of the *Notch1* alleles was deleted in the MDKO, *p57* expression and proliferation were partially rescued (Fig. 7F,G) and the thickness of the trabeculae was reduced compared with that of the MDKO (Fig. 6F). However, *Notch1* deletion did not rescue the defects in trabecular initiation and non-compaction (supplementary material Fig. S5A,B; data not shown). This indicates that NFPs inhibit Notch1 to regulate cardiomyocyte proliferation and trabecular growth/thickness, but not trabecular initiation and compaction. NICD2 overexpression in cardiomyocytes mediated by *αMHC-Cre* results in hypertrabeculation and non-compaction, indicating that Notch2 is involved in compaction and

Development (2014) doi:10.1242/dev.093690

that NFPs might inhibit Notch2 to regulate compaction (Yang et al., 2012). However, many questions regarding the regulation of trabecular morphogenesis by Notch1 and Notch2 remain. Notch2 activity is restricted to trabeculae, where cells are more differentiated, more mature and less proliferative compared with cardiomyocytes in the compact zone, raising a number of questions for future research, such as whether Notch2 inhibits the proliferation of cardiomyocytes and promotes their differentiation to regulate compaction, and what the unique Notch2 downstream targets regulating compaction are. The observation that both *Notch1* deletion (Grego-Bessa et al., 2007) and overexpression (Venkatesh et al., 2008) in endocardial cells reduced trabeculation indicates that further work is needed to reveal how Notch1 regulates trabeculation.

NFPs regulate Notch1 signaling during cardiac development

One of the well-known pathways that NFPs regulate is Notch1 signaling. It has been shown that Numb inhibits Notch1 signaling in *Drosophila* and mammalian cells (Guo et al., 1996; Spana and Doe, 1996; Zhong et al., 1996; McGill and McGlade, 2003; Cheng et al., 2008; McGill et al., 2009; Beres et al., 2011). However, the Numb-Notch1 relationship during vertebrate embryogenesis remains an enigma (Zhong et al., 1996; Petersen et al., 2006). Although the phenotype of the NFP global knockout is similar to that of Notch1 pathway disrupted mutants, leading to the hypothesis that Numb and Notch1 signaling are associated, Notch1 targets were not upregulated in the NFP global knockout during mammalian development, as would be predicted if Numb inhibits Notch1 signaling (Petersen et al., 2006). The exact relationship between Numb and Notch1 during embryogenesis is therefore unclear. Genetic tools to test the interaction between Numb and Notch1 should be applied to reveal the relationship. We used a transgenic Notch reporter line and other assays to clearly show that canonical Notch signaling is upregulated in MDKO hearts. Significantly, deletion of one *Notch1* allele partially rescued the MDKO phenotype, including the expression of *p57*, cardiomyocyte proliferation and trabecular thickness (Fig. 6). This indicates that NFPs regulate trabecular proliferation/growth and thickness via Notch1 signaling.

Notch1 signaling is local and only cells that are adjacent to the ligand will be activated. *Notch1* transcription was highest in endocardial cells and weak in cardiomyocytes. It has been proposed that jagged 1 in cardiomyocytes can activate Notch1 in endocardial cells, so NICD1 is usually detected in endocardial cells (Grego-Bessa et al., 2007). The activated Notch1 signaling in endocardial cells then can enhance cardiomyocyte proliferation by inhibiting *p57* through Bmp10 in the myocardium (Chen et al., 2004; Grego-Bessa et al., 2007; Chen et al., 2013; Luxán et al., 2013). In MDKO hearts, the *Notch1* transcriptional level did not differ from that of the control based on mRNA sequencing and Q-PCR (data not shown), and NICD1 was detected in both endocardial cells and cardiomyocytes, indicating that *Notch1* is expressed in cardiomyocytes and that NFPs are required to inhibit NICD1 in a post-transcriptional manner, consistent with their functions as endocytic proteins. Furthermore, $Nkx2.5^{Cre/+}$-mediated $Notch1^{fl/fl}$ deletion reduced NICD1 to ~46% of control levels based on western blot using lysates of E12.5 ventricles (supplementary material Fig. S6C,D), and presumably the remaining Notch1 protein was contributed by endocardial and epicardial cells. This suggests that Notch1 is expressed in cardiomyocytes at E12.5, considering that $Nkx2.5^{Cre/+}$ is active in all cardiomyocytes and in very few endocardial cells in the ventricles. This is consistent with a previous report that NICD1 is detected in cardiomyocytes in E13.5 and older hearts (Kratsios et al., 2010). We propose that Notch1 in cardiomyocytes is activated by Delta4 (delta-like 4) in the endocardial cells and/or jagged 1 in cardiomyocytes to produce NICD1, which is degraded by NFP-mediated endocytosis and is not detectable in cardiomyocytes in the control hearts. In the cardiomyocytes of MDKO hearts, NFP-mediated NICD1 degradation is abolished, which results in NICD1 accumulation to a detectable level. This NICD1 accumulation in cardiomyocytes activates Notch1-related signaling, including the inhibition of *p57* expression to promote cell proliferation in a myocardium-autonomous manner in the MDKO (Fig. 8A).

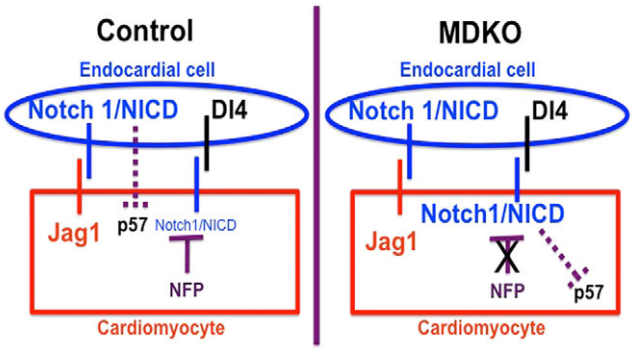

Fig. 8. The deletion of NFPs abolishes NICD1 degradation, resulting in activation of Notch1 signaling. (A) In the control heart, jagged 1 (Jag1) in cardiomyocytes activates Notch1 in endocardial cells to produce NICD1, which in turn can inhibit p57 expression via Bmp10 in cardiomyocytes. Notch1 expression in cardiomyocytes is weak, and can be activated by Delta4 (Dl4) in endocardial cells and/or Jag1 in cardiomyocytes; however, NICD1 will be degraded via NFPs. In NFP-null cardiomyocytes, NICD1 degradation by NFPs is disrupted, resulting in activation of Notch1 and inhibition of p57 expression.

NFPs regulate Notch1-independent signaling pathways

NFPs play a variety of roles during normal and disease conditions in a cell context-dependent manner (Gulino et al., 2010). Numb is an endocytic protein (Santolini et al., 2000), and NFPs execute their functions mainly through their involvement in endocytosis and interaction with other proteins. Numb functions as a component of the adherens junction to regulate cell adhesion and migration in neural epithelium and epicardium (Rasin et al., 2007; Wang et al., 2009; Wu et al., 2010), regulates cancer initiation by controlling the stability of p53 (Colaluca et al., 2008) and Gli1 (Di Marcotullio et al., 2006), regulates neuroblast specification in *Drosophila* SOP cells by inhibiting Notch signaling (Guo et al., 1996), and regulates axon growth in neural cells (Nishimura and Kaibuchi, 2007). Numb also interacts with Notch and Wnt signaling to specify the hemangioblast to the primitive erythroid lineage (Cheng et al., 2008). Of all the pathways with which NFPs interact, the best-studied is the Notch1 pathway. However, suppression of Notch1 did not rescue all the defects of MDKOs, indicating that NFPs function upstream of Notch1-independent signaling pathways to regulate cardiac morphogenesis and cardiac progenitor differentiation.

To reveal the mechanisms that cause the defects in morphogenesis and progenitor differentiation, we examined mRNA deep sequence data. Of the 814 dysregulated genes in the MDKO, 36.9% encode membrane-associated proteins, 30.4% encode glycoproteins and 26.8% encode signal peptides (supplementary material Fig. S7A), indicating that NFPs are involved in multiple signaling pathways, which is consistent with previous findings that Numb is an adaptor protein involved in the endocytosis of multiple proteins (Santolini

Development (2014) doi:10.1242/dev.093690

et al., 2000; Krieger et al., 2013). Indeed, it is possible that NFPs regulate cardiac morphogenesis and progenitor differentiation through the endocytosis of multiple proteins. Analysis of transgenic lines expressing endocytosis-defective Numb might help to determine how NFPs regulate cardiac morphogenesis and progenitor differentiation.

MATERIALS AND METHODS

Mice

Mouse strains *Numb*$^{fl/fl}$, *Numbl*$^{fl/fl}$ (Zilian et al., 2001; Wilson et al., 2007), transgenic Notch reporter (TNR) (Duncan et al., 2005), *Tie2-Cre* (Kisanuki et al., 2001), *Rosa26-mTmG* (mTmG) (Muzumdar et al., 2007), *SM22-Cre* (Holtwick et al., 2002; Boucher et al., 2003), *CMV-Cre* (Schwenk et al., 1995), *Wnt1-Cre* (Danielian et al., 1998), *WT1*^{CreERT2} (Zhou et al., 2008), *αMHC-Cre* (Oka et al., 2006) and *Notch1*$^{fl/fl}$ (Yang et al., 2004) were purchased from Jackson Lab. Dr Robert Schwartz provided *Nkx2.5*$^{Cre/+}$ (Moses et al., 2001) mice. Dr Brian Black provided *Mef2c-Cre* (Verzi et al., 2005). *Nkx2.5*$^{Cre/+}$*; Numb*$^{fl/+}$*; Numbl*$^{fl/fl}$ or *Nkx2.5*$^{Cre/+}$*; Numb*$^{fl/fl}$*; Numbl*$^{fl/+}$ males were mated to *Numb*$^{fl/fl}$*; Numbl*$^{fl/fl}$ females to generate *Nkx2.5*$^{Cre/+}$*; Numb*$^{fl/fl}$*; Numbl*$^{fl/fl}$ designated as MDKO; their sibling embryos without the *Cre* allele are designated as controls. All animal experiments were approved by the Institutional Animal Care and Use Committee (IACUC) at Albany Medical College and performed according to the NIH Guide for the Care and Use of Laboratory Animals.

Paraffin and frozen section immunohistochemistry

Immunohistochemistry, immunofluorescence (IF) and Hematoxylin and Eosin (H&E) staining were performed as described (Lechler and Fuchs, 2005; Mellgren et al., 2008). Primary antibodies were: BrdU (1:50; Becton Dickinson, 347583), collagen IV (1:1000; Chemicon, AB756P), β-tubulin (1:1000; BD Pharmingen, 556321), active caspase 3 (1:100; Cell Signaling, 9661S), WT1 (1:100, DAKO, M3561; or 1:50, Santa Cruz Biotechnology, sc192), PECAM (1:50; BD Pharmingen, 550274), MF20 [1:100; Developmental Studies Hybridoma Bank (DSHB), MF20], β-catenin (1:400; BD Pharmingen, 610153), NICD1 (1:50; Cell Signaling, 4147S), GFP (1:10,000; Abcam, ab290), Isl1 (1:50; DSHB, 39.4D5) and Numb (1:600, Abcam, ab14140; or 1:600, Cell Signaling, 2756s); the third Numb primary antibody was provided by Dr Weimin Zhong at Yale University (1:1000).

mRNA deep sequencing

Total RNA was isolated with Trizol (Invitrogen) from ten E10.5 ventricles from both control and MDKO for each experiment. As an indication of quality, the RNA had an integrity number of 8 or greater by Bioanalyzer (Agilent Technology). Samples for mRNA deep sequencing were prepared according to the manufacturer's protocol (mRNASeq 8-Sample Prep Kit, Illumina). The samples were sequenced by the Microarray Core Facility at the University of Texas, Southwestern Medical Center at Dallas. A HiSeq 2000 system (Illumina) was used for SE-50 sequencing (single-ended 50 bp reads), with over 30×10^6 'reads' per sample. Basic data analysis was performed with CLC-Biosystems Genomic Workbench analysis programs to generate quantitative data for all genes. The quality filtered and trimmed reads were aligned to an annotated mouse reference genome downloaded from the Ensembl Genome Browser. cDNA fragments were mapped back to individual transcripts. After normalization, the RNA-Seq fragment count was used as a measure of relative abundance of transcripts, and CLC BIO measured transcript abundances in reads per kilobase of transcript per million mapped reads (RPKM). The experiment was repeated three times. Relative expression levels of genes (ratio of MDKO to control) with $P<0.05$ were considered significantly different.

Cardiomyocyte isolation

Ventricles (E15.5-17.5) were washed with cold Hank's balanced salt solution, snipped and then digested with warmed 0.2% collagenase B solution. The digestion was repeated four times of four minutes each. The digested mixtures were combined and centrifuged to collect the cardiac cells, which were then plated in a culture dish for 1 hour to allow non-cardiomyocytes to adhere, followed by the transfer of unattached cells to another dish; these last two steps were repeated three times to enrich cardiomyocytes. The cardiomyocyte-enriched cells were cultured and cells that were beating were counted as cardiomyocytes on day four. The enrichment procedure resulted in more than 95% of the cells being cardiomyocytes. The cardiomyocytes were transduced with various viruses or treated with different chemicals for 1, 2 or 3 days. mRNA or proteins were isolated and used for analysis.

Imaging

The following systems were used: for confocal imaging, Zeiss LSM510 META and Zeiss 510 META NLO; for color imaging, Zeiss Observer Z1 with a Hamamatsu ORCA-ER camera; for fluorescence imaging, Zeiss Observer Z1 with an AxioCam MRm camera. 3D images were produced by Zeiss 510 META NLO with 0.9 μm per section and reconstructed with Imaris software (Bitplane).

Cardiomyocyte proliferation assay by BrdU pulse labeling

Pregnant females were intraperitoneally injected with BrdU for 1 hour before embryo harvesting. The proliferation rate was assessed by the percentage of BrdU-positive cells among total cells as described (Wu et al., 2010). Collagen IV was used to stain the basement membrane to distinguish cardiomyocytes from non-cardiomyocytes.

Western blot and co-immunoprecipitation (Co-IP)

Lysates from E12.5 or E13.5 ventricles of each genotype were processed for western blot as described (Mellgren et al., 2008). Lysates from postnatal day (P) 4 hearts were used for Co-IP according to the protocol of uMACS Protein A/G Microbeads (Miltenyi Biotec). Antibodies used for western blots and Co-IP included Numb (1:1000; Cell Signaling, 2756s), NICD1 (1:500; Cell Signaling, 4147s), Notch1 (1:1000; Cell Signaling, 4380s), Notch1 (1:500; Santa Cruz Biotechnology, sc-6014), GFP (1:10,000; Abcam, ab290) and Gapdh (1:1000; Santa Cruz Biotechnology, sc-25778).

RNA isolation and quantitative PCR (Q-PCR)

For Q-PCR analysis, total RNA was isolated from three ventricles for each experiment using Trizol and the RNeasy Micro Kit (Qiagen). The experiments were repeated at least three times for each age. At least 300 ng total RNA was used for reverse transcription (iScript cDNA Synthesis Kit, Bio-Rad). Gene expression was analyzed using standard Q-PCR methods with iTAQ SYBR Green Master Mix on a CFX96 instrument (Bio-Rad). Each sample was run in triplicate and normalized to cyclophilin A. Primer sequences are listed in supplementary material Table S3. Transcription of *Isl1* and *Hey1* was confirmed using two sets of primers.

In situ hybridization

Digoxigenin-labeled RNA probes were made as described (Xu et al., 2009). *In situ* hybridization of whole-mount mouse embryos and paraffin sections was as described (Xu et al., 2011). Briefly, after fixation, embryos were treated with 10 μg/ml proteinase K, refixed in a 0.2% glutaraldehyde/4% paraformaldehyde (PFA) solution, and prehybridized at 65°C for 1 hour. The samples were then transferred into hybridization mix containing 0.5 μg/ml digoxigenin-labeled probes. Post-hybridization washes and antibody incubation were as described (Xu et al., 2009). Color development employed BM Purple solution (Roche).

Trabecular density and thickness quantification and whole-mount IF staining

One in every four sections from E10.5-13.5 hearts was stained with PECAM and MF20 antibodies. At least six sections from the medial part of the heart were quantified for the number of trabeculae per unit length and for the thickness of trabeculae or compact zone in both left and right ventricles. Trabecular thickness was defined as the average thickness of the base, middle and top of an individual trabecula. Compact zone thickness was defined as the average thickness of six different spots in left and right ventricle in each section. The data presented in figures include both left and right ventricles.

Whole embryos were stained as described (Wu et al., 2010). Briefly, whole embryos were fixed for 2 hours in 4% PFA, permeabilized for 8 hours in PBS-Tween 20, blocked with 3% BSA, and then incubated with primary antibody for ~24 hours. After three washes, the embryos were incubated with secondary antibody for 24 hours, followed by washing with PBS. After staining, embryos were cleared in glycerol and then 3D imaged.

Embryoid body (EB) culture and analysis

EB culture was as described (Moore et al., 2004). Briefly, 800 P19Cl6-GFP cells in 20 µl medium (passage number less than 20) were used for each hanging drop culture. Forty-eight hours after hanging drop formation, adenovirus at a multiplicity of infection (MOI) of 100, DAPT at a final concentration of 10 µM, or BafA1 at a final concentration of 0.1 µM, or an equal amount of vehicle (DMSO) mixed in medium was added to the hanging drop without disturbing the cell aggregates. The hanging drops were allowed to grow for another 4 days. Then, the EB or cell aggregates were transferred to culture plates to grow for another 5 days. On day 6, the EB cultures were harvested and dissociated into single cells for flow cytometry analysis or RNA isolation. The percentage of GFP^+ cells was analyzed by FACScan (Becton Dickinson).

Site-directed mutagenesis

Numb mutant variants including $Numb^{DPF/AAA}$ ($NbDPF^m$ or $NbDPF^m$:GFP) and $Numb^{NPF/AAF}$ ($NbNPF^m$), in which DPF and NPF were mutated to AAA and AAF, respectively, were generated by site-directed mutagenesis following protocols provided with the Phusion Site-Directed Mutagenesis Kit (Thermo Scientific). Primers used for $NbDPF^m$ and $NbNPF^m$ generation are (5′-3′, forward and reserve): $Numb^{DPF}$, CCAGGCACCTGCCCA-GTGGCTGCTGCCGAAGCTCAGTGGGCCGCA and AGGGACTTCT-GCATGCCTGTTTCCTGAGGCTAGCCCACCATT; $Numb^{NPF}$, CGTA-CAAATCCTTCTCCTACCGCCGCTTTCTCCAGTGACTTACAGA and CTGCTTGGACTTGCTTTCTAGTGCGGCC.

Ex vivo culture system

The *ex vivo* culture protocol was developed in Dr Brian Black's laboratory. Briefly, embryos lacking the head and tail with the heart exposed to medium were cultured in medium containing Ad-Nb, Ad-GFP or Ad-$NbDPF^m$ for 48 hours. Then, the heart was used for Q-PCR analysis.

Statistics

Data are shown as mean ± s.d. An unpaired two-tailed Student's *t*-test was used for statistical comparison. $P \leq 0.05$ was considered statistically significant.

Lenti RBP-Jk luciferase reporter assay

The Lenti RBP-Jk reporter is a preparation of ready-to-transduce lentiviral particles for monitoring the activity of Notch signaling pathways in virtually any mammalian cell type (Qiagen, CLS-014L). Cardiomyocytes from E16.5-18.5 control or *αMHC-Cre*-mediated NFP knockout hearts were cultured in 48-well plates for 4 days. Then, the cells were infected with Lenti RBP-Jk luciferase and Lenti renilla luciferase, which functions as a control. Seventy-two hours after infection, the lysate was used to measure luciferase activity according to the supplied protocol.

Acknowledgements

We thank Dr Brian Black for helpful comments and critical reading; Drs Eric Olson, Ondine Cleaver, Brian Black and Benoit Bruneau for reagents; the Jay Schneider laboratory for sorting PECAM cells; Dr Christine L. Mummery for the P19Cl6-GFP cell line; Dr Andy Wessels for advice on DMP; Dr Brian Black for establishing the embryo culture system for us; and the M.W. laboratory members for scientific discussion.

Competing interests

The authors declare no competing financial interests.

Author contributions

M.W. designed experiments, analyzed the data and wrote the manuscript. C.Z., H.G., J.L., L.Y., T.M., W.P. and M.W. performed the experiments and analyzed the data. The project was initiated while M.W. was a postdoc in the M.D.T. lab. W.Z., R.J.S., J.S., H.S. and M.D.T. assisted the study.

Funding

This work is supported by Albany Medical College start-up and the American Heart Association [13SDG16920099] to M.W., and by National Heart, Lung, and Blood Institute grants [HL074257] to M.D.T. and [HL049426, HL092510] to H.A.S. Deposited in PMC for release after 12 months.

Supplementary material

Supplementary material available online at
http://dev.biologists.org/lookup/suppl/doi:10.1242/dev.093690/-/DC1

References

Ai, D., Fu, X., Wang, J., Lu, M. F., Chen, L., Baldini, A., Klein, W. H. and Martin, J. F. (2007). Canonical Wnt signaling functions in second heart field to promote right ventricular growth. *Proc. Natl. Acad. Sci. USA* **104**, 9319-9324.

Bao, Z. Z., Bruneau, B. G., Seidman, J. G., Seidman, C. E. and Cepko, C. L. (1999). Regulation of chamber-specific gene expression in the developing heart by Irx4. *Science* **283**, 1161-1164.

Beres, B. J., George, R., Lougher, E. J., Barton, M., Verrelli, B. C., McGlade, C. J., Rawls, J. A. and Wilson-Rawls, J. (2011). Numb regulates Notch1, but not Notch3, during myogenesis. *Mech. Dev.* **128**, 247-257.

Black, B. L. (2007). Transcriptional pathways in second heart field development. *Semin. Cell Dev. Biol.* **18**, 67-76.

Boucher, P., Gotthardt, M., Li, W. P., Anderson, R. G. and Herz, J. (2003). LRP: role in vascular wall integrity and protection from atherosclerosis. *Science* **300**, 329-332.

Breckenridge, R. A., Anderson, R. H. and Elliott, P. M. (2007). Isolated left ventricular non-compaction: the case for abnormal myocardial development. *Cardiol. Young* **17**, 124-129.

Briggs, L. E., Kakarla, J. and Wessels, A. (2012). The pathogenesis of atrial and atrioventricular septal defects with special emphasis on the role of the dorsal mesenchymal protrusion. *Differentiation* **84**, 117-130.

Bruneau, B. G. (2008). The developmental genetics of congenital heart disease. *Nature* **451**, 943-948.

Bruneau, B. G., Bao, Z. Z., Fatkin, D., Xavier-Neto, J., Georgakopoulos, D., Maguire, C. T., Berul, C. I., Kass, D. A., Kuroski-de Bold, M. L., de Bold, A. J. et al. (2001). Cardiomyopathy in Irx4-deficient mice is preceded by abnormal ventricular gene expression. *Mol. Cell. Biol.* **21**, 1730-1736.

Buckingham, M., Meilhac, S. and Zaffran, S. (2005). Building the mammalian heart from two sources of myocardial cells. *Nat. Rev. Genet.* **6**, 826-835.

Cai, C. L., Liang, X., Shi, Y., Chu, P. H., Pfaff, S. L., Chen, J. and Evans, S. (2003). Isl1 identifies a cardiac progenitor population that proliferates prior to differentiation and contributes a majority of cells to the heart. *Dev. Cell* **5**, 877-889.

Calderwood, D. A., Fujioka, Y., de Pereda, J. M., García-Alvarez, B., Nakamoto, T., Margolis, B., McGlade, C. J., Liddington, R. C. and Ginsberg, M. H. (2003). Integrin beta cytoplasmic domain interactions with phosphotyrosine-binding domains: a structural prototype for diversity in integrin signaling. *Proc. Natl. Acad. Sci. USA* **100**, 2272-2277.

Chen, H., Shi, S., Acosta, L., Li, W., Lu, J., Bao, S., Chen, Z., Yang, Z., Schneider, M. D., Chien, K. R. et al. (2004). BMP10 is essential for maintaining cardiac growth during murine cardiogenesis. *Development* **131**, 2219-2231.

Chen, H., Zhang, W., Li, D., Cordes, T. M., Mark Payne, R. and Shou, W. (2009). Analysis of ventricular hypertrabeculation and noncompaction using genetically engineered mouse models. *Pediatr. Cardiol.* **30**, 626-634.

Chen, H., Zhang, W., Sun, X., Yoshimoto, M., Chen, Z., Zhu, W., Liu, J., Shen, Y., Yong, W., Li, D. et al. (2013). Fkbp1a controls ventricular myocardium trabeculation and compaction by regulating endocardial Notch1 activity. *Development* **140**, 1946-1957.

Cheng, X., Huber, T. L., Chen, V. C., Gadue, P. and Keller, G. M. (2008). Numb mediates the interaction between Wnt and Notch to modulate primitive erythropoietic specification from the hemangioblast. *Development* **135**, 3447-3458.

Colaluca, I. N., Tosoni, D., Nuciforo, P., Senic-Matuglia, F., Galimberti, V., Viale, G., Pece, S. and Di Fiore, P. P. (2008). NUMB controls p53 tumour suppressor activity. *Nature* **451**, 76-80.

Conboy, I. M. and Rando, T. A. (2002). The regulation of Notch signaling controls satellite cell activation and cell fate determination in postnatal myogenesis. *Dev. Cell* **3**, 397-409.

Cottage, C. T., Bailey, B., Fischer, K. M., Avitable, D., Collins, B., Tuck, S., Quijada, P., Gude, N., Alvarez, R., Muraski, J. et al. (2010). Cardiac progenitor cell cycling stimulated by pim-1 kinase. *Circ. Res.* **106**, 891-901.

Croquelois, A., Domenighetti, A. A., Nemir, M., Lepore, M., Rosenblatt-Velin, N., Radtke, F. and Pedrazzini, T. (2008). Control of the adaptive response of the heart to stress via the Notch1 receptor pathway. *J. Exp. Med.* **205**, 3173-3185.

Danielian, P. S., Muccino, D., Rowitch, D. H., Michael, S. K. and McMahon, A. P. (1998). Modification of gene activity in mouse embryos in utero by a tamoxifen-inducible form of Cre recombinase. *Curr. Biol.* **8**, 1323-1326.

Di Marcotullio, L., Ferretti, E., Greco, A., De Smaele, E., Po, A., Sico, M. A., Alimandi, M., Giannini, G., Maroder, M., Screpanti, I. et al. (2006). Numb is a suppressor of Hedgehog signalling and targets Gli1 for Itch-dependent ubiquitination. *Nat. Cell Biol.* **8**, 1415-1423.

Duncan, A. W., Rattis, F. M., DiMascio, L. N., Congdon, K. L., Pazianos, G., Zhao, C., Yoon, K., Cook, J. M., Willert, K., Gaiano, N. et al. (2005). Integration of Notch

and Wnt signaling in hematopoietic stem cell maintenance. *Nat. Immunol.* **6**, 314-322.
Frise, E., Knoblich, J. A., Younger-Shepherd, S., Jan, L. Y. and Jan, Y. N. (1996). The Drosophila Numb protein inhibits signaling of the Notch receptor during cell-cell interaction in sensory organ lineage. *Proc. Natl. Acad. Sci. USA* **93**, 11925-11932.
Garg, V., Muth, A. N., Ransom, J. F., Schluterman, M. K., Barnes, R., King, I. N., Grossfeld, P. D. and Srivastava, D. (2005). Mutations in NOTCH1 cause aortic valve disease. *Nature* **437**, 270-274.
Grego-Bessa, J., Luna-Zurita, L., del Monte, G., Bolós, V., Melgar, P., Arandilla, A., Garratt, A. N., Zang, H., Mukouyama, Y. S., Chen, H. et al. (2007). Notch signaling is essential for ventricular chamber development. *Dev. Cell* **12**, 415-429.
Gulino, A., Di Marcotullio, L. and Screpanti, I. (2010). The multiple functions of Numb. *Exp. Cell Res.* **316**, 900-906.
Guo, M., Jan, L. Y. and Jan, Y. N. (1996). Control of daughter cell fates during asymmetric division: interaction of Numb and Notch. *Neuron* **17**, 27-41.
Habara-Ohkubo, A. (1996). Differentiation of beating cardiac muscle cells from a derivative of P19 embryonal carcinoma cells. *Cell Struct. Funct.* **21**, 101-110.
Han, Z. and Bodmer, R. (2003). Myogenic cells fates are antagonized by Notch only in asymmetric lineages of the Drosophila heart, with or without cell division. *Development* **130**, 3039-3051.
Hellström, M., Phng, L. K., Hofmann, J. J., Wallgard, E., Coultas, L., Lindblom, P., Alva, J., Nilsson, A. K., Karlsson, L., Gaiano, N. et al. (2007). Dll4 signalling through Notch1 regulates formation of tip cells during angiogenesis. *Nature* **445**, 776-780.
Hoffman, J. I. and Kaplan, S. (2002). The incidence of congenital heart disease. *J. Am. Coll. Cardiol.* **39**, 1890-1900.
Hoffmann, A. D., Peterson, M. A., Friedland-Little, J. M., Anderson, S. A. and Moskowitz, I. P. (2009). sonic hedgehog is required in pulmonary endoderm for atrial septation. *Development* **136**, 1761-1770.
Holtwick, R., Gotthardt, M., Skryabin, B., Steinmetz, M., Potthast, R., Zetsche, B., Hammer, R. E., Herz, J. and Kuhn, M. (2002). Smooth muscle-selective deletion of guanylyl cyclase-A prevents the acute but not chronic effects of ANP on blood pressure. *Proc. Natl. Acad. Sci. USA* **99**, 7142-7147.
Ilagan, R., Abu-Issa, R., Brown, D., Yang, Y. P., Jiao, K., Schwartz, R. J., Klingensmith, J. and Meyers, E. N. (2006). Fgf8 is required for anterior heart field development. *Development* **133**, 2435-2445.
Ito, T., Kwon, H. Y., Zimdahl, B., Congdon, K. L., Blum, J., Lento, W. E., Zhao, C., Lagoo, A., Gerrard, G., Foroni, L. et al. (2010). Regulation of myeloid leukaemia by the cell-fate determinant Musashi. *Nature* **466**, 765-768.
Jenni, R., Rojas, J. and Oechslin, E. (1999). Isolated noncompaction of the myocardium. *N. Engl. J. Med.* **340**, 966-967.
Kelly, R. G. (2012). The second heart field. *Curr. Top. Dev. Biol.* **100**, 33-65.
Kelly, R. G. and Buckingham, M. E. (2002). The anterior heart-forming field: voyage to the arterial pole of the heart. *Trends Genet.* **18**, 210-216.
Kelly, R. G., Brown, N. A. and Buckingham, M. E. (2001). The arterial pole of the mouse heart forms from Fgf10-expressing cells in pharyngeal mesoderm. *Dev. Cell* **1**, 435-440.
Kisanuki, Y. Y., Hammer, R. E., Miyazaki, J., Williams, S. C., Richardson, J. A. and Yanagisawa, M. (2001). Tie2-Cre transgenic mice: a new model for endothelial cell-lineage analysis in vivo. *Dev. Biol.* **230**, 230-242.
Kratsios, P., Catela, C., Salimova, E., Huth, M., Berno, V., Rosenthal, N. and Mourkioti, F. (2010). Distinct roles for cell-autonomous Notch signaling in cardiomyocytes of the embryonic and adult heart. *Circ. Res.* **106**, 559-572.
Krieger, J. R., Taylor, P., Gajadhar, A. S., Guha, A., Moran, M. F. and McGlade, C. J. (2013). Identification and selected reaction monitoring (SRM) quantification of endocytosis factors associated with Numb. *Mol. Cell. Proteomics* **12**, 499-514.
Kwon, C., Arnold, J., Hsiao, E. C., Taketo, M. M., Conklin, B. R. and Srivastava, D. (2007). Canonical Wnt signaling is a positive regulator of mammalian cardiac progenitors. *Proc. Natl. Acad. Sci. USA* **104**, 10894-10899.
Kwon, C., Cheng, P., King, I. N., Andersen, P., Shenje, L., Nigam, V. and Srivastava, D. (2011). Notch post-translationally regulates β-catenin protein in stem and progenitor cells. *Nat. Cell Biol.* **13**, 1244-1251.
Lechler, T. and Fuchs, E. (2005). Asymmetric cell divisions promote stratification and differentiation of mammalian skin. *Nature* **437**, 275-280.
Li, L., Miano, J. M., Mercer, B. and Olson, E. N. (1996). Expression of the SM22alpha promoter in transgenic mice provides evidence for distinct transcriptional regulatory programs in vascular and visceral smooth muscle cells. *J. Cell Biol.* **132**, 849-859.
Li, H. S., Wang, D., Shen, Q., Schonemann, M. D., Gorski, J. A., Jones, K. R., Temple, S., Jan, L. Y. and Jan, Y. N. (2003). Inactivation of Numb and Numblike in embryonic dorsal forebrain impairs neurogenesis and disrupts cortical morphogenesis. *Neuron* **40**, 1105-1118.
Lin, L., Cui, L., Zhou, W., Dufort, D., Zhang, X., Cai, C. L., Bu, L., Yang, L., Martin, J., Kemler, R. et al. (2007). Beta-catenin directly regulates Islet1 expression in cardiovascular progenitors and is required for multiple aspects of cardiogenesis. *Proc. Natl. Acad. Sci. USA* **104**, 9313-9318.
Luxán, G., Casanova, J. C., Martínez-Poveda, B., Prados, B., D'Amato, G., MacGrogan, D., Gonzalez-Rajal, A., Dobarro, D., Torroja, C., Martinez, F. et al. (2013). Mutations in the NOTCH pathway regulator MIB1 cause left ventricular noncompaction cardiomyopathy. *Nat. Med.* **19**, 193-201.
McBurney, M. W. and Rogers, B. J. (1982). Isolation of male embryonal carcinoma cells and their chromosome replication patterns. *Dev. Biol.* **89**, 503-508.
McCright, B., Gao, X., Shen, L., Lozier, J., Lan, Y., Maguire, M., Herzlinger, D., Weinmaster, G., Jiang, R. and Gridley, T. (2001). Defects in development of the kidney, heart and eye vasculature in mice homozygous for a hypomorphic Notch2 mutation. *Development* **128**, 491-502.
McGill, M. A. and McGlade, C. J. (2003). Mammalian numb proteins promote Notch1 receptor ubiquitination and degradation of the Notch1 intracellular domain. *J. Biol. Chem.* **278**, 23196-23203.
McGill, M. A., Dho, S. E., Weinmaster, G. and McGlade, C. J. (2009). Numb regulates post-endocytic trafficking and degradation of Notch1. *J. Biol. Chem.* **284**, 26427-26438.
Mellgren, A. M., Smith, C. L., Olsen, G. S., Eskiocak, B., Zhou, B., Kazi, M. N., Ruiz, F. R., Pu, W. T. and Tallquist, M. D. (2008). Platelet-derived growth factor receptor beta signaling is required for efficient epicardial cell migration and development of two distinct coronary vascular smooth muscle cell populations. *Circ. Res.* **103**, 1393-1401.
Mishra, R., Vijayan, K., Colletti, E. J., Harrington, D. A., Matthiesen, T. S., Simpson, D., Goh, S. K., Walker, B. L., Almeida-Porada, G., Wang, D. et al. (2011). Characterization and functionality of cardiac progenitor cells in congenital heart patients. *Circulation* **123**, 364-373.
Mizutani, K., Yoon, K., Dang, L., Tokunaga, A. and Gaiano, N. (2007). Differential Notch signalling distinguishes neural stem cells from intermediate progenitors. *Nature* **449**, 351-355.
Mjaatvedt, C. H., Nakaoka, T., Moreno-Rodriguez, R., Norris, R. A., Kern, M. J., Eisenberg, C. A., Turner, D. and Markwald, R. R. (2001). The outflow tract of the heart is recruited from a novel heart-forming field. *Dev. Biol.* **238**, 97-109.
Moore, J. C., Spijker, R., Martens, A. C., de Boer, T., Rook, M. B., van der Heyden, M. A., Tertoolen, L. G. and Mummery, C. L. (2004). A P19Cl6 GFP reporter line to quantify cardiomyocyte differentiation of stem cells. *Int. J. Dev. Biol.* **48**, 47-55.
Moses, K. A., DeMayo, F., Braun, R. M., Reecy, J. L. and Schwartz, R. J. (2001). Embryonic expression of an Nkx2-5/Cre gene using ROSA26 reporter mice. *Genesis* **31**, 176-180.
Mummery, C., Ward, D., van den Brink, C. E., Bird, S. D., Doevendans, P. A., Opthof, T., Brutel de la Riviere, A., Tertoolen, L., van der Heyden, M. and Pera, M. (2002). Cardiomyocyte differentiation of mouse and human embryonic stem cells. *J. Anat.* **200**, 233-242.
Muzumdar, M. D., Tasic, B., Miyamichi, K., Li, L. and Luo, L. (2007). A global double-fluorescent Cre reporter mouse. *Genesis* **45**, 593-605.
Niikura, Y., Tabata, Y., Tajima, A., Inoue, I., Arai, K. and Watanabe, S. (2006). Zebrafish Numb homologue: phylogenetic evolution and involvement in regulation of left-right asymmetry. *Mech. Dev.* **123**, 407-414.
Nishimura, T. and Kaibuchi, K. (2007). Numb controls integrin endocytosis for directional cell migration with aPKC and PAR-3. *Dev. Cell* **13**, 15-28.
Oka, T., Maillet, M., Watt, A. J., Schwartz, R. J., Aronow, B. J., Duncan, S. A. and Molkentin, J. D. (2006). Cardiac-specific deletion of Gata4 reveals its requirement for hypertrophy, compensation, and myocyte viability. *Circ. Res.* **98**, 837-845.
Olson, E. N. (2006). Gene regulatory networks in the evolution and development of the heart. *Science* **313**, 1922-1927.
Park, E. J., Ogden, L. A., Talbot, A., Evans, S., Cai, C. L., Black, B. L., Frank, D. U. and Moon, A. M. (2006). Required, tissue-specific roles for Fgf8 in outflow tract formation and remodeling. *Development* **133**, 2419-2433.
Petersen, P. H., Zou, K., Hwang, J. K., Jan, Y. N. and Zhong, W. (2002). Progenitor cell maintenance requires numb and numblike during mouse neurogenesis. *Nature* **419**, 929-934.
Petersen, P. H., Zou, K., Krauss, S. and Zhong, W. (2004). Continuing role for mouse Numb and Numbl in maintaining progenitor cells during cortical neurogenesis. *Nat. Neurosci.* **7**, 803-811.
Petersen, P. H., Tang, H., Zou, K. and Zhong, W. (2006). The enigma of the numb-Notch relationship during mammalian embryogenesis. *Dev. Neurosci.* **28**, 156-168.
Rasin, M. R., Gazula, V. R., Breunig, J. J., Kwan, K. Y., Johnson, M. B., Liu-Chen, S., Li, H. S., Jan, L. Y., Jan, Y. N., Rakic, P. et al. (2007). Numb and Numbl are required for maintenance of cadherin-based adhesion and polarity of neural progenitors. *Nat. Neurosci.* **10**, 819-827.
Rhyu, M. S., Jan, L. Y. and Jan, Y. N. (1994). Asymmetric distribution of numb protein during division of the sensory organ precursor cell confers distinct fates to daughter cells. *Cell* **76**, 477-491.
Rochais, F., Mesbah, K. and Kelly, R. G. (2009). Signaling pathways controlling second heart field development. *Circ. Res.* **104**, 933-942.
Salcini, A. E., Confalonieri, S., Doria, M., Santolini, E., Tassi, E., Minenkova, O., Cesareni, G., Pelicci, P. G. and Di Fiore, P. P. (1997). Binding specificity and in vivo targets of the EH domain, a novel protein-protein interaction module. *Genes Dev.* **11**, 2239-2249.
Samsa, L. A., Yang, B. and Liu, J. (2013). Embryonic cardiac chamber maturation: trabeculation, conduction, and cardiomyocyte proliferation. *Am. J. Med. Genet. C Semin. Med. Genet.* **163C**, 157-168.
Sanalkumar, R., Dhanesh, S. B. and James, J. (2010). Non-canonical activation of Notch signaling/target genes in vertebrates. *Cell. Mol. Life Sci.* **67**, 2957-2968.
Santolini, E., Puri, C., Salcini, A. E., Gagliani, M. C., Pelicci, P. G., Tacchetti, C. and Di Fiore, P. P. (2000). Numb is an endocytic protein. *J. Cell Biol.* **151**, 1345-1352.
Schwenk, F., Baron, U. and Rajewsky, K. (1995). A cre-transgenic mouse strain for the ubiquitous deletion of loxP-flanked gene segments including deletion in germ cells. *Nucleic Acids Res.* **23**, 5080-5081.
Smith, A. G. (2001). Embryo-derived stem cells: of mice and men. *Annu. Rev. Cell Dev. Biol.* **17**, 435-462.
Snarr, B. S., O'Neal, J. L., Chintalapudi, M. R., Wirrig, E. E., Phelps, A. L., Kubalak, S. W. and Wessels, A. (2007a). Isl1 expression at the venous pole identifies a novel role for the second heart field in cardiac development. *Circ. Res.* **101**, 971-974.

Snarr, B. S., Wirrig, E. E., Phelps, A. L., Trusk, T. C. and Wessels, A. (2007b). A spatiotemporal evaluation of the contribution of the dorsal mesenchymal protrusion to cardiac development. *Dev. Dyn.* **236**, 1287-1294.
Sorkin, A. (2004). Cargo recognition during clathrin-mediated endocytosis: a team effort. *Curr. Opin. Cell Biol.* **16**, 392-399.
Spana, E. P. and Doe, C. Q. (1996). Numb antagonizes Notch signaling to specify sibling neuron cell fates. *Neuron* **17**, 21-26.
Stankunas, K., Hang, C. T., Tsun, Z. Y., Chen, H., Lee, N. V., Wu, J. I., Shang, C., Bayle, J. H., Shou, W., Iruela-Arispe, M. L. et al. (2008). Endocardial Brg1 represses ADAMTS1 to maintain the microenvironment for myocardial morphogenesis. *Dev. Cell* **14**, 298-311.
Traub, L. M. (2003). Sorting it out: AP-2 and alternate clathrin adaptors in endocytic cargo selection. *J. Cell Biol.* **163**, 203-208.
Uemura, T., Shepherd, S., Ackerman, L., Jan, L. Y. and Jan, Y. N. (1989). numb, a gene required in determination of cell fate during sensory organ formation in Drosophila embryos. *Cell* **58**, 349-360.
Ueno, S., Weidinger, G., Osugi, T., Kohn, A. D., Golob, J. L., Pabon, L., Reinecke, H., Moon, R. T. and Murry, C. E. (2007). Biphasic role for Wnt/beta-catenin signaling in cardiac specification in zebrafish and embryonic stem cells. *Proc. Natl. Acad. Sci. USA* **104**, 9685-9690.
Umans, L., Cox, L., Tjwa, M., Bito, V., Vermeire, L., Laperre, K., Sipido, K., Moons, L., Huylebroeck, D. and Zwijsen, A. (2007). Inactivation of Smad5 in endothelial cells and smooth muscle cells demonstrates that Smad5 is required for cardiac homeostasis. *Am. J. Pathol.* **170**, 1460-1472.
Varadkar, P., Kraman, M., Despres, D., Ma, G., Lozier, J. and McCright, B. (2008). Notch2 is required for the proliferation of cardiac neural crest-derived smooth muscle cells. *Dev. Dyn.* **237**, 1144-1152.
Venkatesh, D. A., Park, K. S., Harrington, A., Miceli-Libby, L., Yoon, J. K. and Liaw, L. (2008). Cardiovascular and hematopoietic defects associated with Notch1 activation in embryonic Tie2-expressing populations. *Circ. Res.* **103**, 423-431.
Verdi, J. M., Schmandt, R., Bashirullah, A., Jacob, S., Salvino, R., Craig, C. G., Program, A. E., Lipshitz, H. D. and McGlade, C. J. (1996). Mammalian NUMB is an evolutionarily conserved signaling adapter protein that specifies cell fate. *Curr. Biol.* **6**, 1134-1145.
Verzi, M. P., McCulley, D. J., De Val, S., Dodou, E. and Black, B. L. (2005). The right ventricle, outflow tract, and ventricular septum comprise a restricted expression domain within the secondary/anterior heart field. *Dev. Biol.* **287**, 134-145.
Vincent, S. D. and Buckingham, M. E. (2010). How to make a heart: the origin and regulation of cardiac progenitor cells. *Curr. Top. Dev. Biol.* **90**, 1-41.
Vitelli, F., Morishima, M., Taddei, I., Lindsay, E. A. and Baldini, A. (2002). Tbx1 mutation causes multiple cardiovascular defects and disrupts neural crest and cranial nerve migratory pathways. *Hum. Mol. Genet.* **11**, 915-922.
Waldo, K. L., Kumiski, D. H., Wallis, K. T., Stadt, H. A., Hutson, M. R., Platt, D. H. and Kirby, M. L. (2001). Conotruncal myocardium arises from a secondary heart field. *Development* **128**, 3179-3188.
Wang, Z., Sandiford, S., Wu, C. and Li, S. S. (2009). Numb regulates cell-cell adhesion and polarity in response to tyrosine kinase signalling. *EMBO J.* **28**, 2360-2373.
Ward, C., Stadt, H., Hutson, M. and Kirby, M. L. (2005). Ablation of the secondary heart field leads to tetralogy of Fallot and pulmonary atresia. *Dev. Biol.* **284**, 72-83.
Watanabe, Y., Kokubo, H., Miyagawa-Tomita, S., Endo, M., Igarashi, K., Aisaki, K., Kanno, J. and Saga, Y. (2006). Activation of Notch1 signaling in cardiogenic mesoderm induces abnormal heart morphogenesis in mouse. *Development* **133**, 1625-1634.
Webb, S., Qayyum, S. R., Anderson, R. H., Lamers, W. H. and Richardson, M. K. (2003). Septation and separation within the outflow tract of the developing heart. *J. Anat.* **202**, 327-342.
Weiford, B. C., Subbarao, V. D. and Mulhern, K. M. (2004). Noncompaction of the ventricular myocardium. *Circulation* **109**, 2965-2971.
Wilson, A., Ardiet, D. L., Saner, C., Vilain, N., Beermann, F., Aguet, M., Macdonald, H. R. and Zilian, O. (2007). Normal hemopoiesis and lymphopoiesis in the combined absence of numb and numblike. *J. Immunol.* **178**, 6746-6751.
Wu, B., Zhang, Z., Lui, W., Chen, X., Wang, Y., Chamberlain, A. A., Moreno-Rodriguez, R. A., Markwald, R. R., O'Rourke, B. P., Sharp, D. J. et al. (2012). Endocardial cells form the coronary arteries by angiogenesis through myocardial-endocardial VEGF signaling. *Cell* **151**, 1083-1096.
Wu, M., Kwon, H. Y., Rattis, F., Blum, J., Zhao, C., Ashkenazi, R., Jackson, T. L., Gaiano, N., Oliver, T. and Reya, T. (2007). Imaging hematopoietic precursor division in real time. *Cell Stem Cell* **1**, 541-554.
Wu, M., Smith, C. L., Hall, J. A., Lee, I., Luby-Phelps, K. and Tallquist, M. D. (2010). Epicardial spindle orientation controls cell entry into the myocardium. *Dev. Cell* **19**, 114-125.
Xu, K., Chong, D. C., Rankin, S. A., Zorn, A. M. and Cleaver, O. (2009). Rasip1 is required for endothelial cell motility, angiogenesis and vessel formation. *Dev. Biol.* **329**, 269-279.
Xu, K., Sacharidou, A., Fu, S., Chong, D. C., Skaug, B., Chen, Z. J., Davis, G. E. and Cleaver, O. (2011). Blood vessel tubulogenesis requires Rasip1 regulation of GTPase signaling. *Dev. Cell* **20**, 526-539.
Yang, X., Klein, R., Tian, X., Cheng, H. T., Kopan, R. and Shen, J. (2004). Notch activation induces apoptosis in neural progenitor cells through a p53-dependent pathway. *Dev. Biol.* **269**, 81-94.
Yang, J., Bücker, S., Jungblut, B., Böttger, T., Cinnamon, Y., Tchorz, J., Müller, M., Bettler, B., Harvey, R., Sun, Q. Y. et al. (2012). Inhibition of Notch2 by Numb/Numblike controls myocardial compaction in the heart. *Cardiovasc. Res.* **96**, 276-285.
Zhang, W., Chen, H., Qu, X., Chang, C. P. and Shou, W. (2013). Molecular mechanism of ventricular trabeculation/compaction and the pathogenesis of the left ventricular noncompaction cardiomyopathy (LVNC). *Am. J. Med. Genet. C Semin. Med. Genet.* **163C**, 144-156.
Zhong, W., Feder, J. N., Jiang, M. M., Jan, L. Y. and Jan, Y. N. (1996). Asymmetric localization of a mammalian numb homolog during mouse cortical neurogenesis. *Neuron* **17**, 43-53.
Zhong, W., Jiang, M. M., Weinmaster, G., Jan, L. Y. and Jan, Y. N. (1997). Differential expression of mammalian Numb, Numblike and Notch1 suggests distinct roles during mouse cortical neurogenesis. *Development* **124**, 1887-1897.
Zhou, B., Ma, Q., Rajagopal, S., Wu, S. M., Domian, I., Rivera-Feliciano, J., Jiang, D., von Gise, A., Ikeda, S., Chien, K. R. et al. (2008). Epicardial progenitors contribute to the cardiomyocyte lineage in the developing heart. *Nature* **454**, 109-113.
Zilian, O., Saner, C., Hagedorn, L., Lee, H. Y., Säuberli, E., Suter, U., Sommer, L. and Aguet, M. (2001). Multiple roles of mouse Numb in tuning developmental cell fates. *Curr. Biol.* **11**, 494-501.

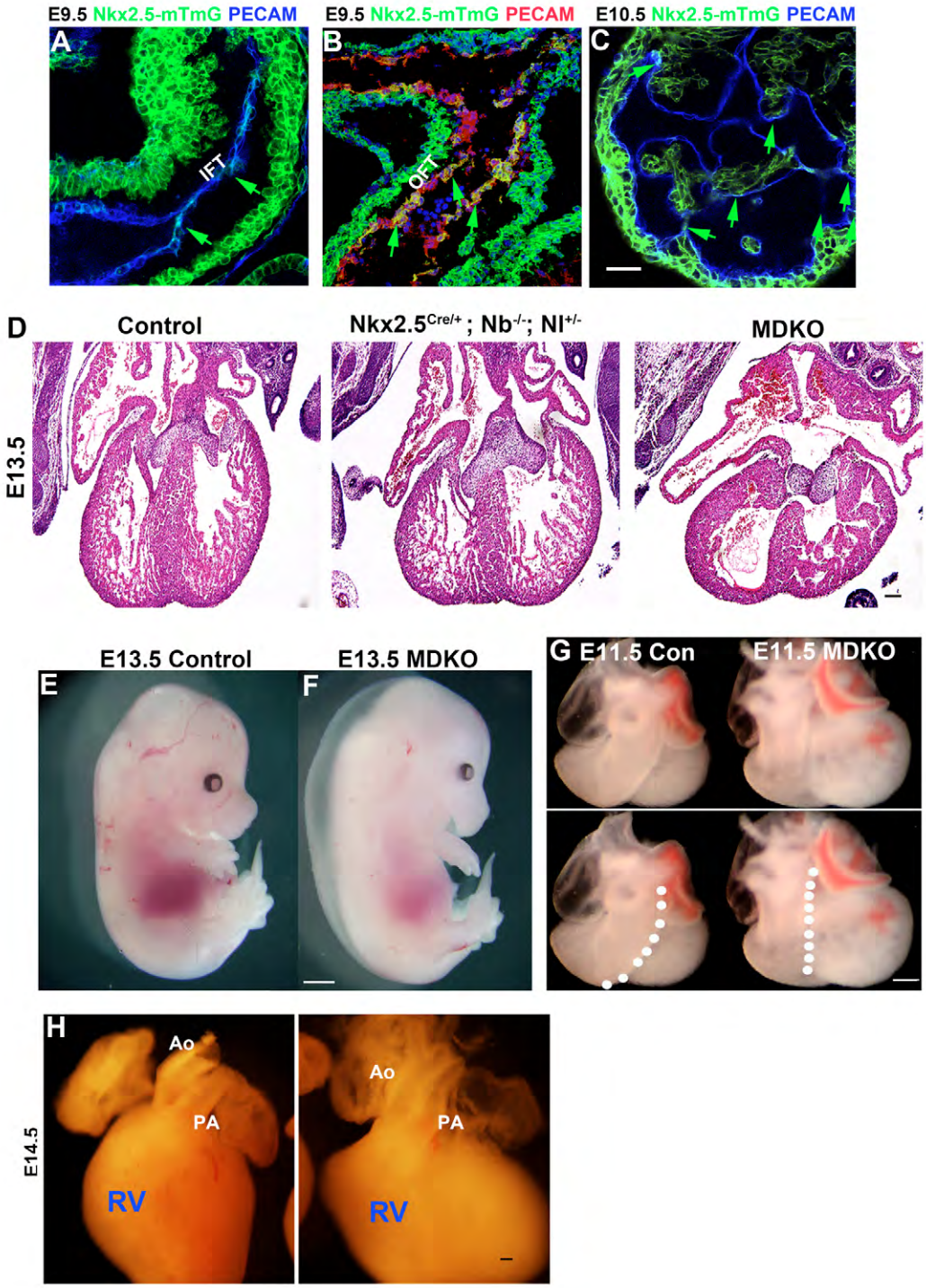

Figure S1. Expression patterns of *Nkx2.5*$^{Cre/+}$ and phenotype of MDKO.

(A-C) Nkx2.5$^{Cre/+}$ was active in cardiomyocytes and endocardial cells of the IFT and OFT, but in very few endocardial cells of ventricles, indicated by green arrows. Sections through the whole heart of E9.5 (A+B) and E10.5 (C) embryos were examined (n=3 for each age). The section in (C) is from a 3D imaged E10.5 whole heart and all of its sections are shown in Movie 1. (D) Heterozygotes heart did not display obvious cardiac defects. (E&F) MDKO embryos displayed edema at E13.5. (G) OFT of MDKO hearts displayed abnormal alignment with ventricles at E11.5. Dotted line delineates the OFT curve. (H) MDKO displayed alignment defect, as both aorta and pulmonary arteries extend from right ventricles. Scale bar in A-C, D, G and H are 20 μm, in E&F are 300μm.

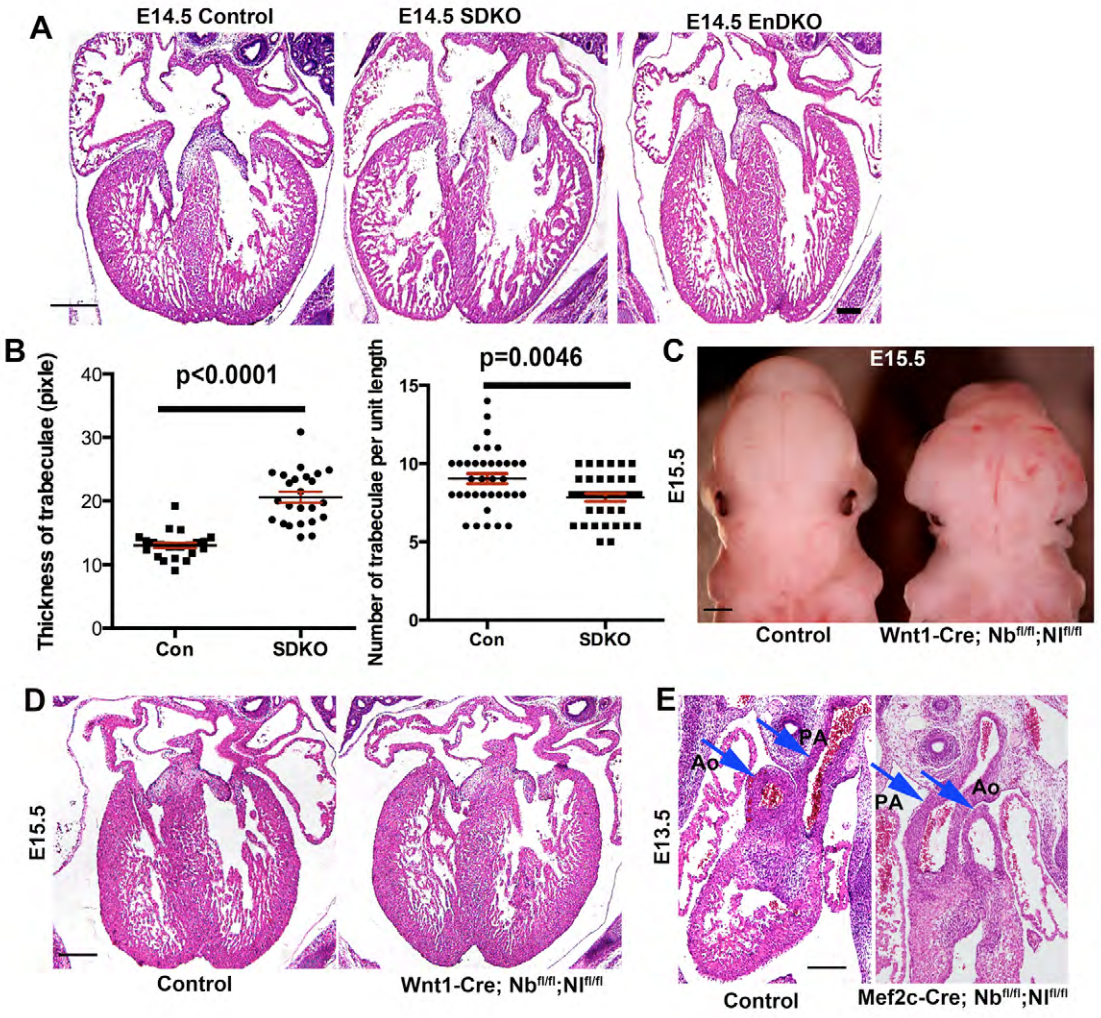

Figure S2. Functions of NFPs in different cardiac cell types.

(A) *SM22-Cre*$^{Tg/0}$; *Numb*$^{fl/fl}$*; Numbl*$^{fl/fl}$ (SDKO) displayed trabeculation defects, showing thicker trabeculae and slight fewer number of trabeculae per unit length. The endocardial cell double knockout (EnDKO) (*Tie2-Cre*$^{Tg/0}$; *Numb*$^{fl/fl}$*; Numbl*$^{fl/fl}$) displayed normal trabeculation and morphogenesis. (B) Shows the quantification of the thickness of trabeculae and the number of trabeculae per unit length in control and SDKO hearts at E14.5. Error bars indicate s.d. (*n=5)*. (C&D) *Wnt1-Cre* mediated NFPs knockout displayed a cranial facial defect, but no cardiac morphogenesis defect. (E) *Mef2c-Cre*-mediated NFPs knockout displayed an OFT alignment defect. Scale bars in A, C, D are 100 μm.

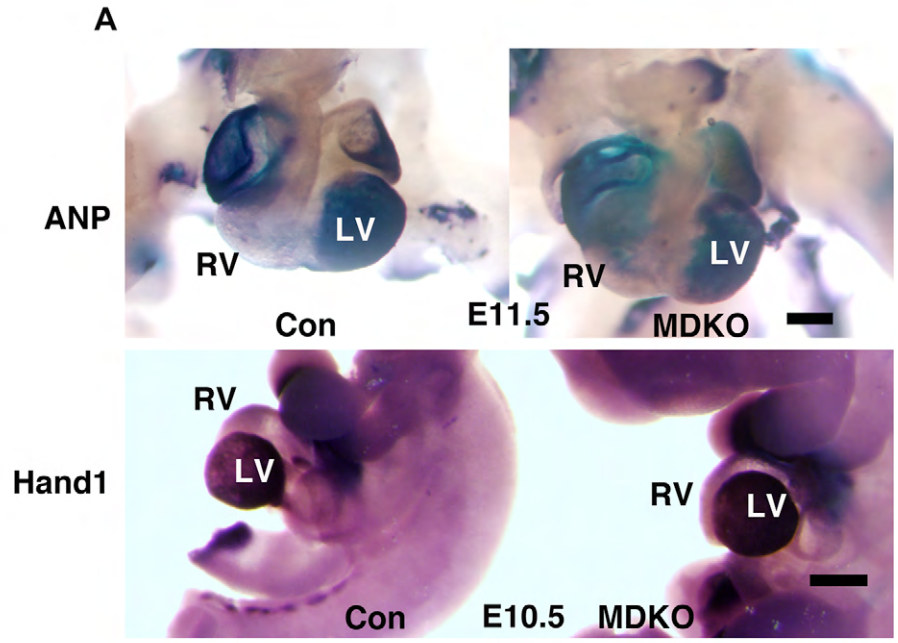

Figure S3. MDKO hearts did not display chamber specification defects.

(A) Expression of *ANP* and *Hand1* in MDKO hearts at E10.5 and E11.5 hearts appears normal based on In situ hybridization. Scale bar in A is 200 μm.

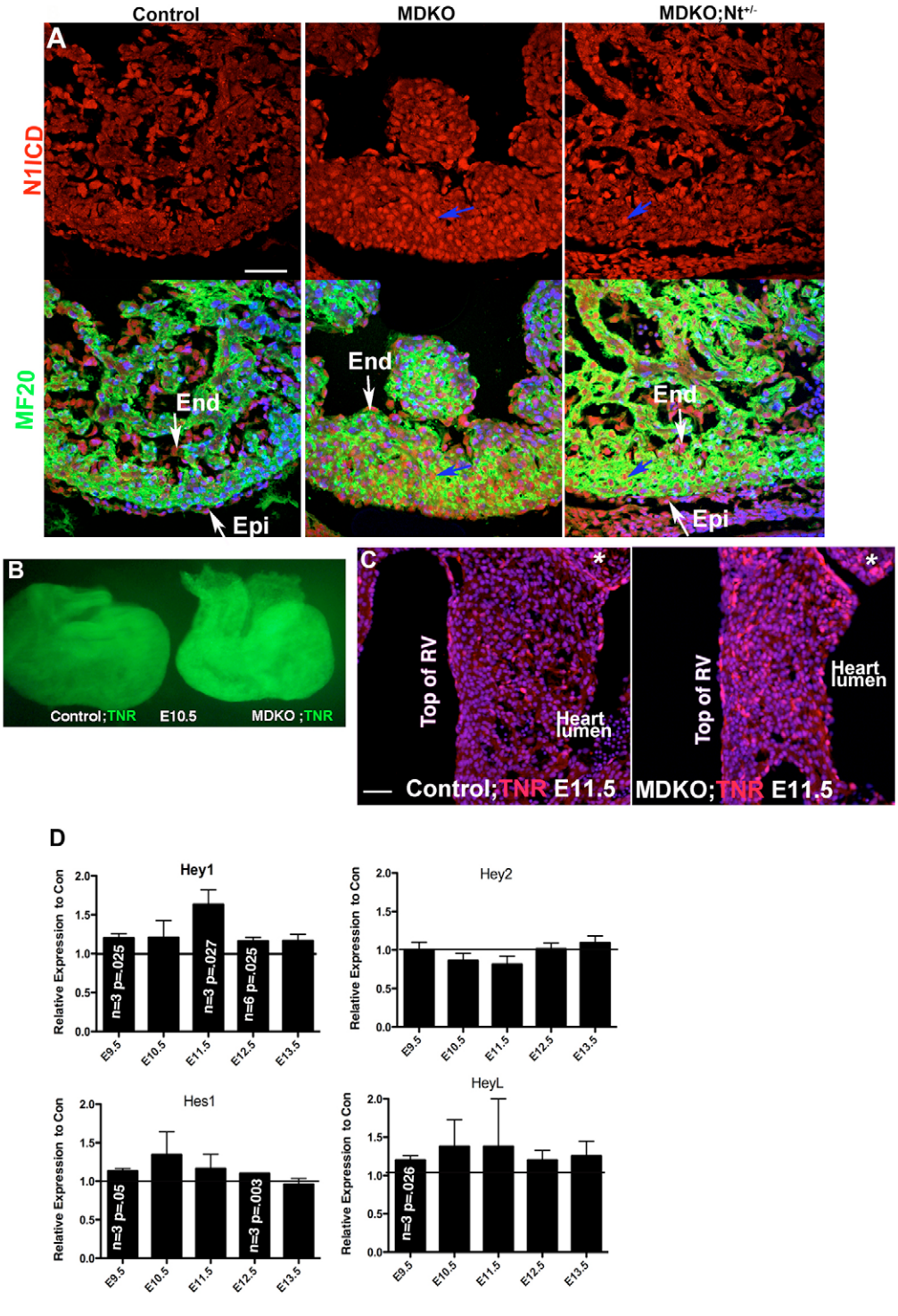

Figure S4. MDKO displayed CBF1 dependent and independent Notch signaling activation.

(A) Control hearts showed NICD1 positive staining in the endocardial cells indicated by white arrows, while MDKO and *MDKO; Nt*$^{+/-}$ hearts additionally displayed NICD1 staining in cardiomyocytes as indicated by blue arrows. (B) Whole heart imaging showed that Notch signaling was up-regulated in MDKO based on the GFP staining of MDKO; TNR heart. (C) MDKO hearts display more TNR positive cells (GFP+) compared to control, but not all cells are TNR positive. (D) Expression of *Hey1* and *Hes1* in MDKO is 1.1 to 1.7-fold higher than control based on Q-PCR at certain ages. Error bars indicate s.d.; *n* values are shown within each bar.

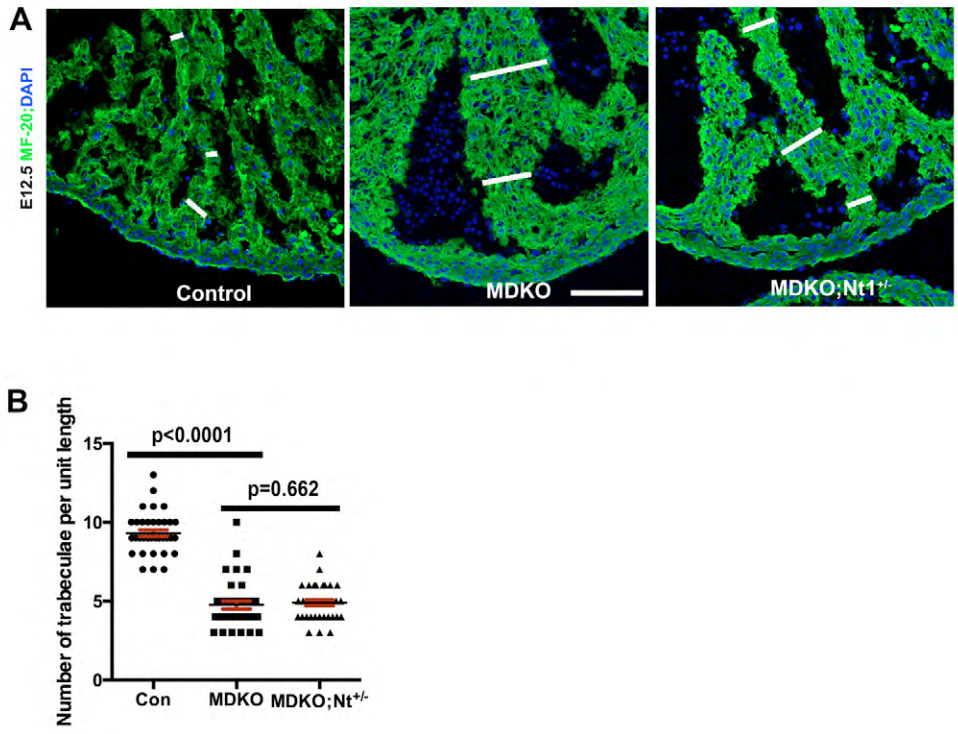

Figure S5. Notch1 suppression decreased the thickness of trabeculae, but not the number of trabeculae per unit length in MDKO.

(A) *MDKO; Nt*$^{+/-}$ displayed less thick trabecula compared to MDKO. (B) Notch1 suppression in MDKO did not increase the number of trabeculae per unit length. Error bars indicate s.d. (*n=5)*. Scale bar in A is 100 μm.

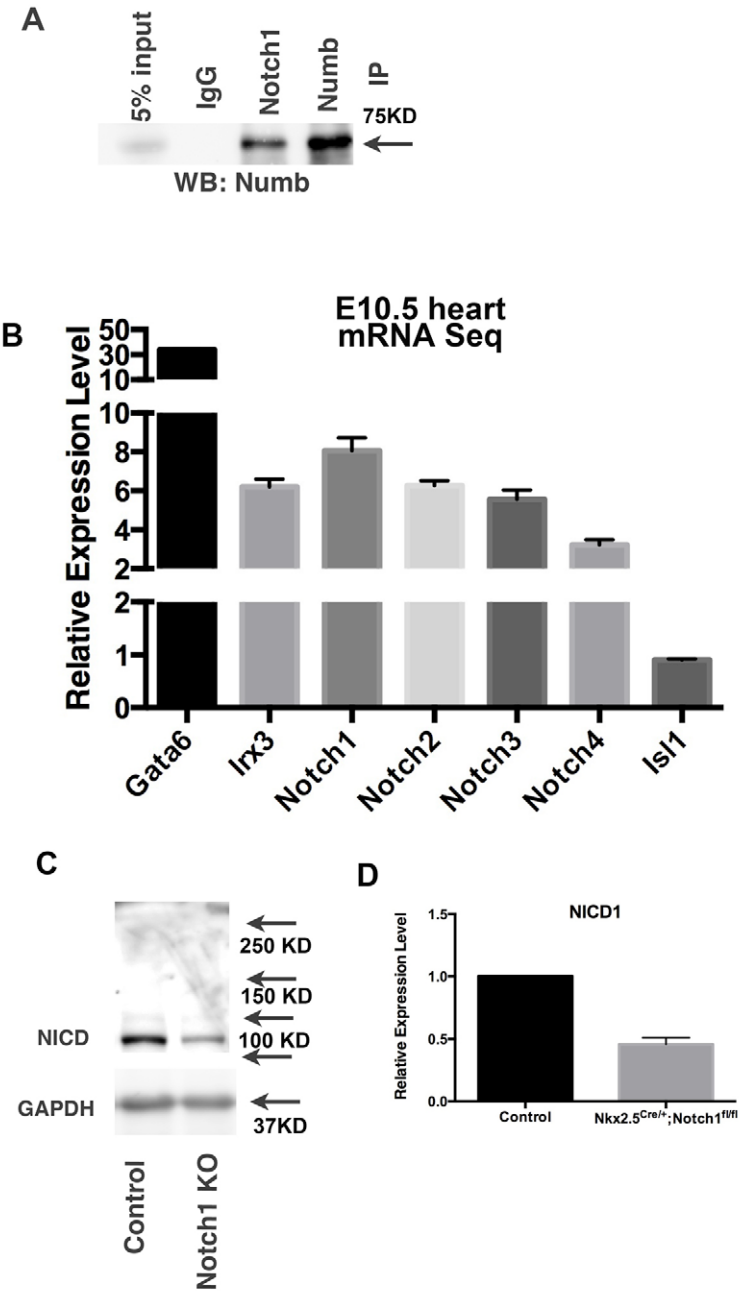

Figure S6. Notch expression in the embryonic heart.

(A) Immunoprecipitation shows that both Numb and Notch1 can pull down Numb from lysate of the heart, in which NFP in endocardial/endothelial cells were deleted via *Nfatc1-Cre*. This indicates that Numb and *Notch1* in cardiomyocytes can bind each other. (B) shows the relative expression of *Gata6*, *Irx3*, *Isl1* and all four Notch receptors based on mRNA deep sequencing using E10.5 hearts. (C&D) *Nkx2.5*$^{Cre/+}$-mediated-*Notch1* deletion reduced the NICD1 to 46% of the control hearts based on Western blot using lysates of E12.5 ventricles. This indicates that the Notch1 is expressed in cardiomyocytes, considering that *Nkx2.5*$^{Cre/+}$ is active in very few endocardial cells in the ventricles.

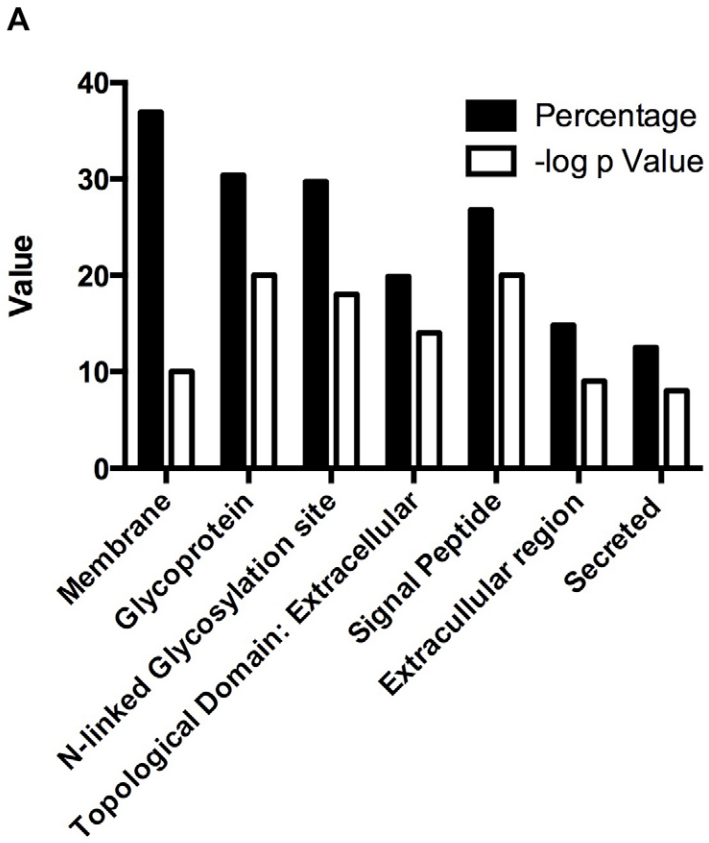

Figure S7. NFPs are involved in multiple signaling pathways during cardiac development.

(A) The percentage of each category of genes that are dysregulated in the MDKO and their–log(p) values are shown. This indicates that NFPs regulate multiple signaling pathways during cardiac morphogenesis.

Movie 1. E10.5 *Nkx2.5$^{Cre/+}$; mTmG* whole hearts were stained with PECAM (blue) and 3D imaged. The movie shows a Z stack of an E10.5 heart with 3 um per section. This movie indicates that very few endocardial cells of the ventricles are Cre active.

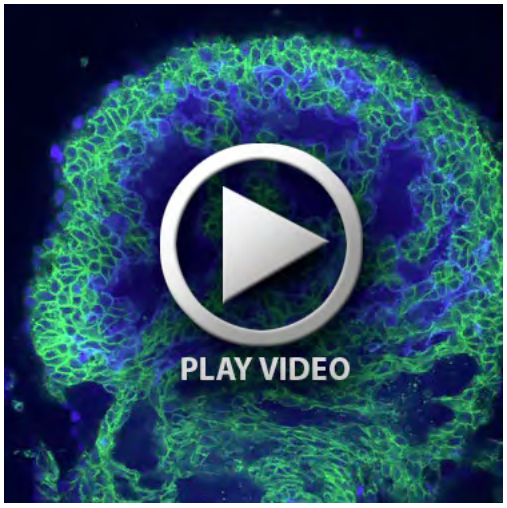

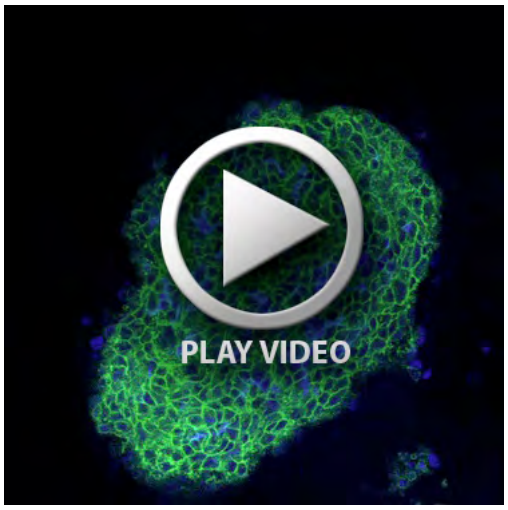

Movies 2 and 3. E10.5 *Nkx2.5$^{Cre/+}$; mTmG* and *MDKO; mTmG* whole hearts were stained with PECAM (blue) and 3D imaged. The movie shows a Z stack of an E10.5 heart with 3 um per section. The movies indicate that the trabecula of MDKO is thicker than that of the control.

Movies 4 and 5. *Mef2c-Cre*-mediated-NFP deletion failed to form Dorsal Mesenchymal Protrusion (DMP) and displayed AVSD. E13.5 *Mef2c-Cre; mTmG* control and knockout hearts were stained with PECAM (Blue) and then 3D imaged. Movies show the Z stack of *Mef2c-Cre* labeled control (Movie 2) and NFPs-null cells (Movie 3) around the DMP region with 3 μm per section. One section of Movie 4/5 is shown in Fig. 3C/D. The genotypes are *Mef2c-Cre; Numb$^{fl/+}$; Numbl$^{fl/+}$; mTmG* for Movie 4 and *Mef2c-Cre; Numb$^{fl/fl}$; Numbl$^{fl/fl}$; mTmG* for Movie 5

Table S1. The results of mRNA deep sequencing. RNA-Seq data of Con vs MDKO at E10.5 including all genes with p-value ≤ 0.05 are listed (15273 genes in total). This experiment was repeated three times and the data of the average of the three were shown. The ratio of MDKO:WT with p-value is presented.

Download Table S1

Table S2. The results of mRNA deep sequencing. Genes whose transcriptional levels were significantly changed are listed. Genes highlighted in red are downregulated, whereas genes highlighted in blue are upregulated.

Download Table S2

Table S3. Primers used for Q-PCR. Both *Hey1* and *Isl1* used two sets of primers.

Gene	Forward	Reverse
Nkx2.5	GACGTAGCCTGGTGTCTCG	GTGTGGAATCCGTCGAAAGT
Hey2	GTGGGGAGCGAGAACAATTA	GTTGTCGGTGAATTGGACCT
Hey1	ACGACATCGTCCCAGGTTTTG	GGTGATCCACAGTCATCTGCAAG
Hey1	CATGAAGAGAGCTCACCCAGA	CGCCGAACTCAAGTTTCC
Hes1	ACACCGGACAAACCAAAGAC	CGCCTCTTCTCCATGATAGG
HeyL	CTGAATTGCGACGATTGGT	GCAAGACCTCAGCTTTCTCC
Hes5	CCAAGGAGAAAAACCGACTG	TGCTCTATGCTGCTGTTGATG
cyclophilin	GGAGATGGCACAGGAGGAA	GCCCGTAGTGCTTCAGCTT
Jag1	GAGGCGTCCTCTGAAAAACA	ACCCAAGCCACTGTTAAGACA
Wnt2	CCTGATGAACCTTCACAACAAC	TCTTGTTTCAAGAAGCGCTTTAC
Tanni2	CAGGATGGGAGATGAGGAGA	TCTGGAGCATCACACTCTTCAG
Gata4	GGAAGACACCCCAATCTCG	CATGGCCCCACAATTGAC
Gata5	CCTTCGACAGCAGCATCC	TCCTCCAAGAAGTCAGGTACG
Gata6	GGTCTCTACAGCAAGATGAATGG	TGGCACAGGACAGTCCAAG
Isl1	AGCAACCCAACGACAAAACT	CCATCATGTCTCTCCGGACT
Isl1	CCACAAGCAGCCGGAGAAGAC	GAGGGTTGGCGGCATAGCAG
Tbx2	GAACGGCCGTCGGGAGAAAAG	TGGGGGAGGGCGGTGGTT
Tbx1	TTTGTGCCCGTAGATGACAA	CTCGGCCAGGTGTAGCAG
Tbx3	TTGCAAAGGGTTTTCGAGAC	TGCAGTGTGAGCTGCTTTCT
Tbx5	CGAAGTGGGCACAGAGATG	CACCTTCACTTTGTAACTAGGAAACA
Hand1	CAAGCGGAAAAGGGAGTTG	GTGCGCCCTTTAATCCTCTT
Hand2	GGAGAAGAGGAAGAAAGAGCTGA	ATGAGGCCCTACTGCTTGAG
Mef2c	TCTGCCCTCAGTCAGTTGG	CGTGGTGTGTTGTGGGTATC
Myh7	CGCATCAAGGAGCTCACC	CTGCAGCCGCAGTAGGTT
Myh6	CGCATCAAGGAGCTCACC	CCTGCAGCCGCATTAAGT
Vcam1	TGGTGAAATGGAATCTGAACC	CCCAGATGGTGGTTTCCTT
Numb	CCACATCAGTGGCAGACAGA	TTCTACGTGGCCGAGGTACT
cyclin D1	TCTTTCCAGAGTCATCAAGTGTG	GACTCCAGAAGGGCTTCAATC
Numbl	CTGCAGCTTCCCTGTTAGGT	TCTTCACAAACGTGCATTCC
Bmp10	TGGTGAGGGATAGACACATTG	CGGAGCTTCAAGAACGAAGA
Irx5	ACAGAAGCCCGAGGACAAG	AAAATCCGAGTCGCTGAGG
Irx3	AAAAGTTACTCAAGACAGCTTTCCA	CGATTTAAAAATGGTTGAAAAGTTAAG
Hop	ACCACGCTGTGCCTCATC	GCGCTGCTTAAACCATTTCT

p57	CAGGACGAGAATCAAGAGCA	GCTTGGCGAAGAAGTCGT
ANF	CACAGATCTGATGGATTTCAAGA	CCTCATCTTCTACCGGCATC
Irx4	AGGGCTATGGCAACTACGTG	CTTGGACTCGAAGCTGTTCA
FoxH1	TTCCTCTAATCGGTGCTTCC	AGCAGGAATCAGGCTCACAT
Cxcl12	CTGTGCCCTTCAGATTGTTG	TAATTTCGGGTCAATGCACA
Nrg1	GTTAGGAAACGACAGTGCCTCT	TTCAGTTGAGGCTGACATGC